we generally performed MRI for the purpose of screening for SCI in this study. Patients with type 1 diabetes, patients with macroalbuminuria (as defined later) and undergoing renal replacement therapy, pregnant women and patients with infectious or malignant diseases were excluded. Those who had clinical and laboratory missing data were also excluded. Type 2 diabetes was diagnosed according to the criteria of the World Health Organization definition.[19]

Participants underwent a routine medical history, physical examination and blood sampling. Information regarding smoking and family history of cardiovascular disease was obtained using a standard questionnaire. Smoking history was classified as either current smoker or non-smoker. Physical examination included blood pressure measurement and anthropometry; laboratory examinations included hemoglobin A1C, serum lipids and creatinine and urinary albumin excretion.

History of cerebrovascular disease was defined as earlier history of transient ischemic attack and/or stroke. History of coronary artery disease was defined as the presence of any of the following conditions: angina pectoris diagnosed by coronary angiography or myocardial scintigraphy, earlier myocardial infarction or earlier revascularization. History of peripheral artery disease was defined as earlier lower extremity peripheral artery disease according to American College of Cardiology/American Heart Association 2005 guideline.[20]

Measurements

Cranial MRI scans were performed using a 1.5-T MR system (GyroScan Intere 1.5T master, Philips or MRT-2001/P3 excelart, Toshiba). T1- (repetition time, 400 ms; echo time, 10 ms) and T2-weighted images (repetition time, 3500 ms; echo time, 90 ms) were obtained in the transverse plane with 7-mm thick sections. SCI was defined by cranial MRI examinations as an area of low-signal intensity measuring at least 3 mm on T1-weighted images, which was also visible as a hyperintense lesion on T2-weighted images, according to the clinical guidelines by the Japanese Society for Detection of Asymptomatic Brain Disease.[21] Hyperintense punctuate lesions evident only on T2-weighted images were excluded from the diagnosis of SCI. In each case, SCI was diagnosed by consensus of two neuroradiologists at the Tokyo Women's Medical University Hospital.

Classification of the degree of urinary albumin was assessed according to American Diabetes Association criteria, on the basis of at least two out of three albumin-to-creatinine ratio (ACR) measurements obtained from first morning urine specimens.[7] Normo-, micro- and macroalbuminuria were defined as an ACR <30, 30–299 and $\geqslant 300\,mg\,g^{-1}$, respectively. Glomerular filtration rate (GFR) was estimated using the following modified three-variable equation for Japanese: $GFR=194\times SCr^{-1.094}\times age^{-0.287}$ ([if female]$\times$0.739) $ml\,min^{-1}\,1.73\,m^{-2}$.[22] The primary end point was defined as transition from normo- to microalbuminuria or micro- to macroalbuminuria, confirmed on at least two consecutive urinary ACR measurements to reduce misclassification.

Hemoglobin A1C was measured by high-performance liquid chromatography (normal range: 4.3–5.8%), and total cholesterol and high-density lipoprotein cholesterol were determined enzymatically. Low-density lipoprotein cholesterol was calculated using the Friedewald equation when serum triglycerides level was <400 mg per 100 ml.[23]

Statistical analyses

Data were expressed as percentage, arithmetic mean ± s.d. or geometric mean with 95% confidence interval (CI), as appropriate according to data distribution. Triglycerides and ACR were logarithmically transformed because of skewed distributions. For statistical analyses, Student's *t*-test or χ^2 test were conducted according to the appropriate situation. The cumulative incidence of the primary end point was estimated using the Kaplan–Meier method. Risk estimates for reaching the end point were calculated using univariate and multivariate Cox proportional hazard model analyses. The following variables were incorporated as covariates: age, gender, duration of diabetes, presence of proliferative diabetic retinopathy, smoking status, body mass index, systolic and diastolic blood pressure, use of renin–angiotensin system inhibitors (angiotensin-converting enzyme inhibitors and angiotensin type 1-receptor blockers), antiplatelet agents, statins, hemoglobin A1C, triglycerides, high-density lipoprotein cholesterol, low-density lipoprotein cholesterol, hemoglobin, uric acid, eGFR and urinary ACR at baseline. Prognostic factors were selected using the stepwise procedure, specifying the significant levels for entering another explanatory variable into the model as 0.25, and that for removing an explanatory variable from the model as 0.15. A *P*-value <0.05 was considered significant. All statistical analyses were performed using the SAS version 9.13 (SAS Institute, Cary, NC, USA).

RESULTS

A total of 366 type 2 diabetic patients had sufficient baseline and follow-up data to qualify for inclusion, including 149 women and 217 men, with a mean (± s.d.) age of 64 ± 10 years (range: 29–89 years). At baseline, 246 patients had normoalbuminuria and 120 patients had microalbuminuria. SCI was detected in 171 patients (46.7%). Patients with SCI were older and had higher systolic blood pressure and urinary albumin excretion and lower body mass index, hemoglobin levels and eGFR than patients without SCI (Table 1).

During a median follow-up period of 3.9 years (range: 0.3–6.0 years), 23 normoalbuminuric and 24 microalbuminuric patients reached the primary end point.

Twelve (8.5%) of 141 patients without SCI and 11 (10.5%) of 105 patients with SCI progressed from normo- to microalbuminuria. The progression from micro- to macroalbuminuria was observed in 6 (11.1%) of 54 patients without SCI and 18 (27.3%) of 66 patients with SCI. In contrast, the regression of nephropathy (from micro- to

Table 1 Demographic and laboratory data in type 2 diabetic patients with and without SCI at baseline

	Without SCI (N=195)	*With SCI (N=171)*	P-*value*[a]
Age (years)	61 ± 10	69 ± 8	<0.001
Gender (% men)	61.0	57.3	0.470
Current smoker (%)	22.6	14.6	0.053
Diabetes duration (years)	15 ± 10	15 ± 9	0.761
Body mass index ($kg\,m^{-2}$)	25.1 ± 4.0	24.1 ± 3.4	0.011
Systolic blood pressure (mm Hg)	134 ± 19	139 ± 19	0.008
Diastolic blood pressure (mm Hg)	77 ± 12	75 ± 14	0.112
Proliferative diabetic retinopathy (%)	16.4	18.7	0.563
Medication (%)			
OHA/insulin	54.9/39.5	55.6/40.9	0.778
RAS blockers (%)	45.1	55.6	0.048
Antiplatelet agents (%)	34.9	54.4	<0.001
Statins (%)	33.3	34.5	0.814
Hemoglobin A1C (%)	8.1 ± 1.6	7.9 ± 1.6	0.316
Triglycerides ($mmol\,l^{-1}$)[b]	1.41 (1.31–1.52)	1.36 (1.26–1.48)	0.508
HDL cholesterol ($mmol\,l^{-1}$)	1.31 ± 0.41	1.35 ± 0.43	0.414
LDL cholesterol ($mmol\,l^{-1}$)	3.01 ± 0.85	2.97 ± 0.77	0.604
Uric acid ($\mu mol\,l^{-1}$)	304 ± 73	300 ± 85	0.649
Hemoglobin ($g\,l^{-1}$)	141 ± 13	135 ± 15	<0.001
ACR ($mg\,g^{-1}$)[b]	18 (15–21)	24 (20–29)	0.007
<30 (%)	72.3	61.4	0.027
30–299 (%)	27.7	38.6	0.027
Serum creatinine ($\mu mol\,l^{-1}$)	65.6 ± 14.9	72.1 ± 22.5	0.001
eGFR ($ml\,min^{-1}\,1.73\,m^{-2}$)	77.9 ± 17.0	68.6 ± 16.8	<0.001

Abbreviations: ACR, albumin-to-creatinine ratio; CI, confidence interval; GFR, glomerular filtration rate; HDL, high-density lipoprotein; LDL, low-density lipoprotein; OHA, oral hypoglycemic agent; RAS, rennin-angiotensin system; SCI, silent cerebral infarction.
Data are expressed as mean ± s.d., geometric mean (95% CI), or percentage.
[a]Student's *t*-test or χ^2 test,
[b]Geometric mean.

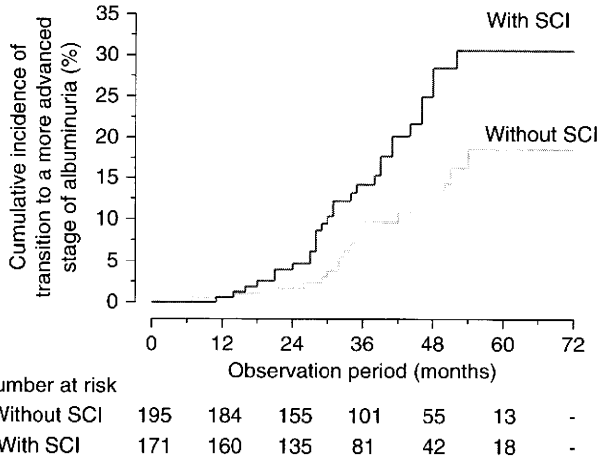

Number at risk							
Without SCI	195	184	155	101	55	13	-
With SCI	171	160	135	81	42	18	-

Figure 1 Cumulative incidence of the end point (transition to a more advanced stage of albuminuria) in Japanese type 2 diabetic patients with and without SCI. The difference between Kaplan–Meier estimates for the two groups was statistically significant by log-rank test (P=0.020).

normoalbuminuria) was also observed in 12 (10.0%) of 120 microalbuminuric patients during the follow-up period. The cumulative incidence of the primary end point, that is progression to micro- or macroalbuminuria, was significantly higher for patients with SCI than those without SCI (log-rank test, P=0.020; Figure 1). In the univariate Cox proportional hazard model, the hazard ratio of the end point for patients with SCI *vs.* those without SCI was 1.98 (95% CI=1.10–3.56, P=0.023). This statistical association remained significant even after adjustment for other covariates using the stepwise multivariate Cox regression analysis (hazard ratio=2.02, 95% CI=1.09–3.72, P=0.025). Other covariates finally included in the multivariate analysis were SCI, logarithmically transformed ACR, hemoglobin and proliferative diabetic retinopathy. SCI (hazard ratio=2.02, 95% CI=1.09–3.72, P=0.025), logarithmically transformed ACR (hazard ratio=4.61, 95% CI=2.65–8.02, $P<0.001$) and hemoglobin (hazard ratio=0.843, 95% CI=0.71–0.94, P=0.016) were selected as significant covariates.

DISCUSSION

Albuminuria is a strong risk factor for cardiovascular disease;[3,4] however, limited data are available on the opposite relation, for example whether patients with cardiovascular disease have a great risk of incident albuminuria.[18,24] In this study, we observed a higher incidence of the development and progression of nephropathy in type 2 diabetic subjects with SCI than without. This association remained significant after adjustment for covariates. To the best of our knowledge, this is the first study to show the significant association between SCI and the development or progression of albuminuria in a cohort of diabetic patients.

Concerning the cardio-renal association in diabetic patients, as we discussed earlier,[17] albuminuria and cardiovascular disease share numerous risk factors that may help to explain the observed relationship between SCI and nephropathy in this study. Hemodynamic and anatomical aspects of renal and cerebral small vessels share many similarities,[25,26] and a common pathogenesis may contribute to both SCI and incident nephropathy in patients with type 2 diabetes. Another possible mechanism that may contribute to the association of SCI with albuminuria involves asymmetric dimethylarginine, an endogenous inhibitor of nitric oxide synthase, which was shown to be associated with prevalent SCI in the Framingham offspring study.[27] We have recently shown that elevated plasma asymmetric dimethylarginine is a significant predictor of the development and progression of nephropathy in diabetic patients.[28] Furthermore, Hashimoto *et al.*[29] cross-sectionally showed that large artery stiffness (pulse wave velocity) is an important factor, which explains the association between cerebral lacunar infarction and albuminuria. Stiffening of large arteries increases the pulsatile stress because of increased aortic characteristic impedance and early return of wave reflection, and it could eventually lead to microvascular damage of the brain (SCI) and kidneys (albuminuria). Therefore, the cerebro-renal association (SCI and albuminuria) in this study may be at least in part explained by stiffening of large arteries. Further studies are needed to better understand the common pathogenesis of SCI and albuminuria in diabetic patients.

In contrast to our study, Uzu *et al.*[18] recently showed that SCI was not associated with the incidence of nephropathy, but progression to renal failure in Japanese diabetic patients. The differences of the impact of SCI on the renal outcomes between the study[18] and ours are unclear. One possible explanation may be due to the differences in the patient characteristics. In our study, the prevalence of patients with microalbuminuria was nearly equal to that in the population-based study in Japan,[30] but smaller than that of the study by Uzu *et al.*[18] In addition, patients in this study were older, probably explaining the higher prevalence of SCI because aging is a strong predictor of SCI.[8] Further large prospective studies are needed to elucidate the association between SCI and incident albuminuria in diabetic patients.

Our study population was ethnically and socially homogeneous and, therefore, may not be generalizable to other ethnic groups or the general population. Furthermore, cranial MRIs in this study were mainly performed for the purpose of screening for SCI, yielding a strong selection bias. Therefore, the higher prevalence of SCI in this study may be overestimated. Second, the follow-up period is relatively short. Third, we never determined the impact of SCI on the progression to end-stage renal disease. Nevertheless, this study is the first to reveal the significant association between SCI and incident albuminuria in diabetic patients and may facilitate identification of diabetic patients carrying a higher risk of progression of nephropathy.

In conclusion, SCI may be a predictor of the development and progression of nephropathy in Japanese patients with type 2 diabetes.

ABBREVIATIONS

CKD, chronic kidney disease; SCI, silent cerebral infarction; MRI, magnetic resonance imaging; ACR, albumin-to-creatinine ratio; ADMA, asymmetric dimethylarginine; OHA, oral hypoglycemic agent; RAS, renin–angiotensin system.

CONFLICT OF INTEREST

The authors declare no conflict of interest.

1 National Kidney Foundation. K/DOQI clinical practice guidelines for chronic kidney disease: evaluation classification stratification. Part 4. Definition and classification of stages of chronic kidney disease. *Am J Kidney Dis* 2002; **39**(Suppl 1): S46–S75.
2 Go AS, Chertow GM, Fan D, McCulloch CE, Hsu CY. Chronic kidney disease and the risks of death, cardiovascular events, and hospitalization. *N Eng J Med* 2004; **351**: 1296–1305.
3 So WY, Kong AP, Ma RC, Ko GT, Kong AP, Zhao H, Luk AO, Lam CW, Ho CS, Tong PC, Chan JC. Glomerular filtration rate, cardiorenal end points, and all-cause-mortality in type 2 diabetic patients. *Diabetes Care* 2006; **29**: 2046–2052.
4 Arnlöv J, Evans JC, Meigs JB, Wang TJ, Fox CS, Levy D, Benjamin EJ, D'Agostino RB, Vasan RS. Low-grade albuminuria and incidence of cardiovascular disease events in nonhypertensive and nondiabetic individuals: the Framingham Heart Study. *Circulation* 2005; **16**: 969–975.

5 Babazono T, Nyumura I, Toya K, Hayashi T, Ohta M, Suzuki K, Kiuchi Y, Iwamoto Y. Higher levels of urinary albumin excretion within the normal range predict faster decline in glomerular filtration rate in diabetic patients. *Diabetes Care* 2009; **32**: 1518–1520.
6 Caramori ML, Fioretto P, Mauer M. The need for early predictors of diabetic nephropathy risk: is albumin excretion rate sufficient? *Diabetes* 2000; **49**: 1399–1408.
7 American Diabetes Association. Nephropathy in diabetes. *Diabetes Care* 2004; **27** (Suppl 1): S79–S83.
8 Vermeer SE, Koudstaal PJ, Oudkerk M, Hofman A, Breteler MM. Prevalence and risk factor of silent brain infarcts in the population-based Rotterdam Scan Study. *Stroke* 2002; **33**: 21–25.
9 Lee SC, Park SJ, Ki HK, Gwon HC, Chung CS, Byun HS, Shin KJ, Shin MH, Lee WR. Prevalence and risk factors of silent cerebral infarction in apparently normal adults. *Hypertension* 2000; **36**: 73–77.
10 Fisher CM. Lacnar strokes and infarcts: a review. *Neurology* 1982; **32**: 871–876.
11 Bruno A, Rosenberg GA. The spectrum of lacnar infarction in the elderly. *Clin Geriatr Med* 1991; **7**: 443–453.
12 Kobayashi S, Okada K, Koide H, Bokura H, Yamaguchi S. Subcortical silent brain infarction as a risk factor for clinical stroke. *Stroke* 1997; **28**: 1932–1939.
13 Naganuma T, Uchida J, Tsuchida K, Takemoto Y, Tatsumi S, Sugimura K, Nakatani T. Silent cerebral infarction predicts vascular events in hemodialysis patients. *Kidney Int* 2005; **67**: 2434–2439.
14 Vermeer SE, Prins ND, den Heijer T, Hofman A, Koudstaal PJ, Breteler MM. Silent MRI infarcts and the risk of dementia and cognitive decline. *N Engl J Med* 2003; **348**: 1215–1222.
15 Wada M, Nagasawa H, Kurita K, Koyama S, Arawaka S, Kawanami T, Tajima K, Daimon M, Kato T. Microalbuminuria is a risk factor for cerebral small vessel disease in community-based elderly subjects. *J Neurol Sci* 2007; **15**: 27–34.
16 Nakamura T, Kawagoe Y, Matsuda T, Ueda Y, Ebihara I, Koide H. Silent cerebral infarction in patients with type 2 diabetic nephropathy. Effects of antiplatelet drug dilazep dihydrochloride. *Diabetes Metab Res Rev* 2005; **21**: 39–43.
17 Bouchi R, Babazono T, Nyumura I, Toya K, Hayashi T, Ohta M, Hanai K, Kiuchi Y, Suzuki K, Iwamoto Y. Is reduced estimated glomerular filtration rate a risk factor for stroke in patients with type 2 diabetes? *Hypertens Res* 2009; **32**: 381–386.
18 Uzu T, Kida Y, Shirahashi N, Harada T, Yamauchi A, Nomura M, Isshiki K, Araki SI, Sugimoto T, Koya D, Haneda M, Kashiwagi A, Kikkara R. Cerebral microvascular disease predicts renal failure in type 2 diabetes. *J Am Soc Nephrol* 2010; **21**: 520–526.
19 Alberti KGMM, Zimmet P, for the WHO consultation. Definition, diagnosis, and classification of diabetes mellitus and its complications, part 2: diagnosis and classification of diabetes mellitus provisional report of a WHO consultation. *Diabet Med* 1998; **15**: 539–553.
20 Hirsch AT, Haskal ZJ, Hertzer NR, Bakal CW, Creager MA, Halperin JL, Hiratzka LF, Murphy WR, Olin JW, Puschett JB, Rosenfield KA, Sacks D, Stanley JC, Taylor Jr LM, White CJ, White J, White RA, Antman EM, Smith Jr SC, Adams CD, Anderson JL, Faxon DP, Fuster V, Gibbons RJ, Hunt SA, Jacobs AK, Nishimura R, Ornato JP, Page RL, Riegel B. ACC/AHA 2005 Practice Guidelines for the Management of Patients With Peripheral Arterial Disease (Lower Extremity, Renal, Mesenteric, and Abdominal Aortic). *Circulation* 2006; **113**: e436–e465.
21 Sasaki M, Hirai T, Taoka T, Higano S, Wakabayashi C, Matsusue E, Ida M. Discriminating between silent cerebral infarction and deep white matter hyperintensity using combinations of three types of magnetic resonance images: a multicenter observer performance study. *Neuroradiology* 2008; **50**: 753–758.
22 Matsuo S, Imai E, Horio M, Yasuda Y, Tomita K, Nitta K, Yamagata K, Tomino Y, Yokoyama H, Hishida A, Collaborators developing the Japanese equation for estimated GFR. Revised equations for estimated GFR from serum creatinine in Japan. *Am J Kidney Dis* 2009; **53**: 982–992.
23 Friedewald WT, Levy RI, Fredrickson DS. Estimation of the concentration of low-density lipoprotein cholesterol in plasma, without use of the preparative ultracentrifuge. *Clin Chem* 1972; **18**: 499–502.
24 Retnakaran R, Cull CA, Thorne KI, Adler AI, Holman RR; UKPDS Study Group. Risk factors for renal dysfunction in type 2 diabetes: U.K. Prospective Diabetes Study 74. *Diabetes* 2006; **55**: 1832–1839.
25 O'Rourke MF, Safar ME. Relationship between aortic stiffening and microvascular disease in brain and kidney: cause and logic of therapy. *Hypertension* 2005; **46**: 200–204.
26 Ito S, Nagasawa T, Abe M, Mori T. Strain vessel hypothesis: a viewpoint for linkage of albuminuria and cerebro-cardiovascular risk. *Hypertens Res* 2009; **32**: 115–121.
27 Pikula A, Böger RH, Beiser AS, Maas R, DeCarli C, Schwedhelm E, Himali JJ, Schulze F, Au R, Kelly-Hayes M, Kase CS, Vasan RS, Wolf PA, Seshadri S. Association of plasma ADMA levels with MRI markers of vascular brain injury: Framingham offspring study. *Stroke* 2009; **40**: 2959–2964.
28 Hanai K, Babazono T, Nyumura I, Toya K, Tanaka N, Tanaka M, Ishii A, Iwamoto Y. Asymmetric dimethylarginine is closely associated with the development and progression of nephropathy in patients with type 2 diabetes. *Nephrol Dial Transplant* 2009; **24**: 1884–1888.
29 Hashimoto J, Aikawa T, Imai Y. Large artery stiffening as a link between cerebral lacunar infarction and renal albuminuria. *Am J Hypertens* 2008; **21**: 1304–1309.
30 Yokoyama H, Kawai K, Kobayashi M, Japan Diabetes Clinical Data Management Study Group. Microalbuminuria is common in Japanese type 2 diabetic patients: a nationwide survey from the Japan Diabetes Clinical Data Management Study Group (JDDM 10). *Diabetes Care* 2007; **30**: 989–992.

Connective tissue growth factor (CTGF/CCN2) is increased in peritoneal dialysis patients with high peritoneal solute transport rate

Makoto Mizutani, Yasuhiko Ito, Masashi Mizuno, Hayato Nishimura, Yasuhiro Suzuki, Ryohei Hattori, Yoshihisa Matsukawa, Masaki Imai, Noelynn Oliver, Roel Goldschmeding, Jan Aten, Raymond T. Krediet, Yukio Yuzawa and Seiichi Matsuo

Am J Physiol Renal Physiol 298:F721-F733, 2010. First published 16 December 2009; doi:10.1152/ajprenal.00368.2009

Am J Physiol Renal Physiol 298: F721–F733, 2010.
First published December 23, 2009; doi:10.1152/ajprenal.00368.2009.

Connective tissue growth factor (CTGF/CCN2) is increased in peritoneal dialysis patients with high peritoneal solute transport rate

Makoto Mizutani,[1] Yasuhiko Ito,[1] Masashi Mizuno,[1] Hayato Nishimura,[1] Yasuhiro Suzuki,[1] Ryohei Hattori,[2] Yoshihisa Matsukawa,[2] Masaki Imai,[3] Noelynn Oliver,[4] Roel Goldschmeding,[5] Jan Aten,[6] Raymond T. Krediet,[7] Yukio Yuzawa,[1] and Seiichi Matsuo[1]

Departments of [1]Nephrology and Renal Replacement Therapy and [2]Urology, Nagoya University Graduate School of Medicine, Nagoya; [3]Department of Immunology, Nagoya City University Graduate School of Medical Sciences, Nagoya, Japan; [4]FibroGen, Inc., San Francisco, California; [5]Department of Pathology, University Medical Center Utrecht, Utrecht; and Departments of [6]Pathology and [7]Nephrology, Academic Medical Center, University of Amsterdam, Amsterdam, The Netherlands

Submitted 30 June 2009; accepted in final form 10 December 2009

Mizutani M, Ito Y, Mizuno M, Nishimura H, Suzuki Y, Hattori R, Matsukawa Y, Imai M, Oliver N, Goldschmeding R, Aten J, Krediet RT, Yuzawa Y, Matsuo S. Connective tissue growth factor (CTGF/CCN2) is increased in peritoneal dialysis patients with high peritoneal solute transport rate. *Am J Physiol Renal Physiol* 298: F721–F733, 2010. First published December 23, 2009; doi:10.1152/ajprenal.00368.2009.— Peritoneal fibrosis (PF) is an important complication of peritoneal dialysis (PD) therapy that often occurs in association with peritoneal high transport rate and ultrafiltration failure (UFF). To study the possible pathogenic role of connective tissue growth factor (CTGF) in the relationship of PF and UFF, dialysate CTGF contents (n = 178) and tissue CTGF expression (n = 61) were investigated by ELISA, real-time PCR, immunohistochemistry, and in situ hybridization. CTGF production with and without TGF-β_1 stimulation in human peritoneal mesothelial cells (HPMC) from the spent patients' peritoneal dialysate (n = 32) was studied in vitro. The dialysate-to-plasma ratio for creatinine (D/P Cr) was positively correlated to dialysate CTGF concentration and estimated local peritoneal production of CTGF. CTGF mRNA expression was 11.4-fold higher in peritoneal membranes with UFF than in pre-PD renal failure peritoneum and was correlated with thickness of the peritoneum. CTGF protein and mRNA were detected in mesothelium and in fibroblast-like cells. In cultured HPMC, TGF-β_1-induced expression of CTGF mRNA was increased at 12 and 24 h and was correlated with D/P Cr. In contrast, bone morphogenic protein-4 mRNA expression was inversely correlated with D/P Cr. Our results suggest that high peritoneal transport state is associated with fibrosis and increased peritoneal CTGF expression and production by mesothelial cells, which can be stimulated by TGF-β_1. Dialysate CTGF concentration could be a biomarker for both peritoneal fibrosis and membrane function. Functional alteration of mesothelial cells may be involved in progression of peritoneal fibrosis in high transport state.

TGF-β; BMP-4; BMP-7; fibrosis; ultrafiltration failure

LONG-TERM PERITONEAL DIALYSIS (PD) treatment is accompanied by functional and histopathological alterations in the peritoneum (10, 14, 28). The characteristic feature of chronic peritoneal damage in PD treatment is decreased ultrafiltration capacity associated with submesothelial fibrosis, accumulation of extracellular matrix, and neoangiogenesis leading to a large vessel peritoneal surface area (49). The decrease in ultrafiltration capacity seen after prolonged PD is one of the important reasons for its discontinuation (22). The pathogenesis of peritoneal fibrosis is attributed to a combination of bioincompatible factors in dialysate, including high osmolality, high glucose (10), advanced glycation products (47) and glucose degradation products (48), uremic inflammation (49), and acute peritonitis with inflammation (11, 12, 40). Importantly, peritoneal fibrosis/sclerosis often occurs in association with high transport rate and ultrafiltration failure (UFF). The mechanism of these interactions between peritoneal fibrosis and UFF, which may become a target to prevent the peritoneal damage, is still not clear. In addition, there is no biomarker that reflects both conditions.

Connective tissue growth factor (CTGF; CCN-2) is a 349 amino acid cysteine-rich polypeptide belonging to the CCN (CTGF/Cyr61/Nov) family. CTGF was first identified in conditioned media of endothelial cells as a 36- to 38-kDa polypeptide containing chemotactic activity toward fibroblasts. The CCN family consists of six regulatory proteins, which participate in diverse biological processes such as angiogenesis and wound healing and are involved in control of migration, cell proliferation and differentiation, and epithelial-to-mesenchymal transition (EMT) (7, 39). CTGF is highly expressed during development of various fibrotic disorders and has been acknowledged as one of the key growth factors in extracellular matrix production and other profibrotic activities mediated by transforming growth factor (TGF)-β (25, 52, 53). In patients with Type 1 diabetic nephropathy, we observed that plasma CTGF is an independent predictor of end-stage renal disease and mortality (34) and that urinary CTGF excretion is correlated with clinical markers of renal disease (33). CTGF was also detected in peritoneal fluid of patients undergoing peritoneal dialysis (57). However, since these latter studies used small numbers of patients, they were not sufficiently powered to draw conclusions on the potential use of CTGF as biomarker in PD patients and the possible pathophysiological role of CTGF in peritoneal transport. Therefore, we investigated CTGF expression in human peritoneal fibrosis and peritoneal transport dysfunction using human peritoneal tissue, dialysate, and cultured mesothelial cells from continuous ambulatory peritoneal dialysis (CAPD) patients with varying rates of peritoneal transport.

SUBJECTS AND METHODS

Patients and Experimental Design

All studies were approved by the Ethics Committee for Human Research of the Faculty of Medicine, Nagoya University (approval no.

Address for reprint requests and other correspondence: Y. Ito, Dept. of Nephrology, Nagoya Univ., 65 Tsurumai-cho, Showa-ku, Nagoya 466-8550, Japan (e-mail: yasuito@med.nagoya-u.ac.jp).

298, peritoneal fluid experiment; no. 299, peritoneal tissues experiment), and all patients provided informed consent prior to participation in the study.

Peritoneal transport of CTGF in PD patients. CTGF concentration in peritoneal effluent was measured in overnight dwelled (8.79 ± 2.10 h) samples collected from 155 PD patients (63 women, 92 men) treated between January 2005 to December 2007 at the Department of Nephrology and Renal Replacement Therapy of Nagoya University Hospital (Nagoya, Japan) and at affiliated hospitals including Handa Municipal Hospital, Nagoya Kyoritsu Hospital, Kounan-Kousei Hospital, and Anjo-Kosei Hospital. The mean age of all patients was 58.4 ± 13.7 (range 27 to 89) yr and the mean duration of CAPD treatment was 41.2 ± 36.1 (range 1 to 180) mo. Diabetic nephropathy was the cause of end-stage renal disease in 52 PD patients (33.5%). All patients were free from peritonitis for at least 1 mo prior to the study, and patients with other diseases, such as liver or lung diseases and malignancy, were excluded. Patients undergoing combination therapy (hemodialysis + PD) were not included in this study. Peritoneal transport was assessed in 144 PD patients by ratios of creatinine concentrations in dialysate and plasma (D/P Cr) and the average value was 0.65 ± 0.15 (range 0.20 to 0.96). Correlation between CTGF concentration in PD effluent and D/P Cr was analyzed in 144 PD patients. A separate study using 23 stable PD patients of Nagoya University Hospital (14 men and 9 women, mean age 52.8 ± 11.5 yr, mean PD treatment duration 30.2 ± 25.3 mo) was designed to estimate the proportion of PD effluent CTGF that is derived from local production in the peritoneal cavity. CTGF, β_2-microglobulin, IgG, and α_2-macroglobulin content were measured in blood (Na_2EDTA plasma or serum) and dialysate samples at 4 h of peritoneal equilibration tests (PET). The fast PET was performed using 2.27% glucose-based dialysis solutions (Dianeal-N PD-4, Baxter) as described by Twardowski et al. (45). Serum creatinine levels were measured enzymatically on an automated analyzer (JCA-BM6050, JEOL, Tokyo, Japan). β_2-Microglobulin was determined by microparticle enzyme immunoassay β_2-microglobulin kit (Denka, Niigata, Japan). Albumin, immunoglobulin G, and α_2-macroglobulin concentrations were measured by turbidimetric immunoassay with albumin kit (Shinotest, Sagamihara, Japan), IgG kit (Nittobo, Tokyo, Japan), and N antiserum to human α_2-macroglobulin (Dade Behring Marburg, Marburg, Germany), respectively. Na_2EDTA plasma of 15 healthy controls (6 men and 9 women, mean age 40.9 ± 7.7 yr) were used to measure levels of CTGF in healthy individuals.

CTGF mRNA expression and correlation with histology of peritoneum. We obtained 61 peritoneal tissue samples from 35 PD patients and 26 pre-PD controls (chronic renal failure patients who needed PD catheter insertion because of advanced renal failure). Among the 35 PD patients, 7 were regarded as having impaired ultrafiltration capacity (UFF), which was defined by use of more than four hypertonic bags (2.27% glucose, 3.86% glucose or icodexitrin) in each 24 h to maintain fluid balance (17); 5 patients were peritonitis positive; and 23 patients (incidental) had their catheters removed because of transplantation, mental disorders, severe exit site infection, or difficulty to do the bag exchanges (Table 1). Correlation of CTGF mRNA expression with peritoneal membrane thickness and number of vessels was evaluated.

Table 2. *Patient profiles of the culture studies*

	PD Duration (< 2 yr)	All Patients
Male	18	25
Female	7	7
Total	25	32

	D/P Cr	PD Duration (< 2 yr)	All Patients
Low	~0.49	11	15
Low average	~0.5–0.64		
High average	~0.65–0.81	14	17
High	~0.82		

D/P Cr; ratio of creatinine concentrations in dialysate and plasma, an index of the peritoneal transport.

CTGF production in human mesothelial cells. Human peritoneal mesothelial cells (HPMC) were isolated from spent glucose-based peritoneal dialysis fluid (Dianeal-N PD-4, pH 6.5–7.5, Baxter, Tokyo, Japan) taken from 32 clinically stable patients (Table 2) and cultured by use of a modified method described previously (5, 26). Basal and TGF-β_1 induced CTGF mRNA expression in both HPMC and human mesothelial cell line, Met-5A, were studied as detailed below.

Processing of Biopsy Samples and Morphological Analysis

Samples of parietal peritoneum were biopsied in the standard manner and processed as reported previously (17, 35, 49). The tissue samples were fixed with 10% buffered formalin overnight, routinely processed for light microscopy, and embedded in paraffin. The 4-μm-thick sections were cut and stained with hematoxylin and eosin and Masson's trichrome. Before analysis of peritoneal thickness, each specimen was assessed for size, site, and direction of the peritoneum, then judged adequate as described by Honda et al. (17). In 40 of 61 samples, thickness and the number of the vessels could be measured. To assess the extent of peritoneal thickening, the submesothelial compact zone was identified as the peritoneal fibrosis between basal border of the surface mesothelial cells and upper border of the peritoneal adipose tissues (17, 49). We measured peritoneal thickness at five random points using a Zeiss Z1 microscope and Axiovision Windows software version 4.4 (Carl Zeiss, Oberkochen, Germany), and mean thickness was calculated.

IHC and ISH for CTGF and α-SMA

In total 44 tissue samples from 32 PD patients and 12 predialysis control patients were performed for immunohistochemistry (IHC). The 4-μm-thick sections of formalin-fixed, paraffin-embedded tissues were deparaffinated and rehydrated. The slides were boiled in 0.04 M citrate, 0.12 M, phosphate, pH 5.8, for 10 min at 100°C. After washing, sections were incubated in 0.3% hydrogen peroxide in methanol to block endogenous peroxidase and were incubated in 10% normal goat serum (Dako, Glostrup, Denmark) in PBS to block nonspecific binding. Afterward, the sections were incubated with mouse monoclonal anti-human CTGF antibody (FibroGen, San Fran-

Table 1. *Peritoneal biopsy cases evaluated for CTGF mRNA expression*

	Control	UFF	Peritonitis	Incidental
n	26	7	5	23
Male	17	3	5	13
Female	9	4	0	10
Age, yr	62.0 ± 12.8	55.9 ± 11.6	72.5 ± 12.8	60.8 ± 13.2
Duration of treatment, yr	0	9.4 ± 6.6	2.4 ± 1.8	3.7 ± 3.0
Average thickness of peritoneum, μm	157.9 ± 62.1	308.6 ± 129.2	432.1 ± 322.8	155.7 ± 93.1

Values are means ± SD. CTGF, connective tissue growth factor; Control, peritoneal tissues were taken at time when a peritoneal dialysis (PD) catheter was inserted because of renal failure; UFF, cases of ultra-filtration failure; incidental, peritoneal tissues were taken when the catheter was removed because of reasons other than UFF.

cisco, CA) at 1 μg/ml in PBS for 16 h at 4°C, followed by reaction with a conjugate of polyclonal goat anti-mouse IgG antibody and horseradish peroxidase-labeled polymer (Histofine Simple Stain, Nichirei, Tokyo, Japan) as a secondary reagent. Enzyme activity was detected by use of a 3,3′-diaminobenzidine tetrahydrochloride liquid system (Dako) (30, 32). Immunostaining for α-smooth muscle actin (α-SMA) was performed by using mouse monoclonal α-SMA antibody (1A3; Dako) as we described previously (16–18). Counterstaining with hematoxylin was done on the IHC sections of CTGF and α-SMA.

In situ hybridization (ISH) to detect CTGF mRNA was performed on the 10% buffered formalin-fixed paraffin-embedded human peritoneal biopsy tissues by using previously described methods (19, 20). Counterstaining with hematoxylin was not performed on the ISH sections.

ELISA for CTGF

CTGF protein was measured in Na_2EDTA-plasma and peritoneal dialysate (PD fluid) samples. Samples were frozen at the time of collection, stored at −80°C, and not subjected to freeze-thaw cycles. CTGF was detected by sandwich ELISAs using monoclonal antibodies against distinct epitopes on the NH_2-terminal and COOH-terminal halves of human CTGF (FibroGen) with similar protocols as we have described previously (33, 34). The same preparation of full-length recombinant human CTGF (rhCTGF, FibroGen) in appropriate matrixes was used for standards in all assays, making the results of the different ELISAs comparable and obviating the need to equalize concentration of the different CTGF forms by molarity. Low-, medium-, and high-concentration rhCTGF quality control samples, prepared by using matrixes similar to that of the experimental samples, were included in each assay plate to identify quantitation and detection limits. Acceptable coefficients of variation for the quality control replicates were set to be ≤20% for medium and high concentration quality control samples and ≤25% for the lowest concentration quality control samples. In some of the PD fluid analyses, values were extrapolated from the calibration curve to report "low" values that are above the lower limit of detection (LOD) but below the lower limit of quantitation (LLOQ). The assays used detected NH_2-terminal half fragments of CTGF (N-CTGF, *domains 1* and *2*) and/or full-length CTGF (W-CTGF, consisting of *domains 1–4*). We determined sample concentrations of CTGF N-half fragments plus W-CTGF with CTGF ELISAs that use monoclonal antibodies directed against epitopes in *domains 1* and *2*. For these assays, the LOD for PD fluid was 1.6 ng/ml and the LLOQ was ~14 ng/ml. For Na_2EDTA plasma, the LLOQ = 4.7 ng/ml. We determined sample concentrations of W-CTGF with a CTGF ELISA that uses monoclonal antibodies directed against epitopes in *domains 1* and *3*. The LOD for PD fluid was 3.2 ng/ml and the LLOQ was 4.7 ng/ml. For Na_2EDTA plasma, the LLOQ = 4.7 ng/ml. The intra- and interassay coefficients of variation were 6 and 20%, respectively.

Calculations for Local Peritoneal Production of CTGF

Local peritoneal production of CTGF was defined as the difference between the measured and expected dialysate concentration calculated from the peritoneal transport line of each patient by using the methods by Zweers et al. (59, 60). The peritoneal transport line was computed for each patient based on the least squares regression analysis of the dialysate-to-serum (D/S) ratio of β_2-microglobulin [molecular weight (MW) 11,800 Da], albumin (MW 69,000), IgG (MW 150,000) and α_2-macroglobulin (MW 820,000) and their MWs when plotted on a double logarithmic scale. The expected amount of CTGF protein (MW 22,000 as described below) transported from the circulation to the peritoneal cavity was estimated by using the peritoneal transport line of each patient. The slope of this line represents the size selectivity of the peritoneal membrane. "Local peritoneal CTGF production index" of each individual is calculated from the difference between measured dialysate-to-plasma ratio for CTGF (D/P CTGF) and expected D/P CTGF values transported from the circulation to the peritoneal cavity.

Cell Culture Study

A human mesothelial cell line (Met-5A), which was derived after transfection with pRSV-T plasmid from pleural fluid of noncancerous patients, was purchased from the American Type Culture Collection (ATCC, Manassas, VA) and maintained according to ATCC guidelines. Briefly, Met-5A cells were grown in Medium 199 containing Earle's BSS, L-glutamine, and sodium bicarbonate (Sigma, Tokyo, Japan) supplemented with 10% fetal bovine serum (FBS, Sigma), 20 mM HEPES (Dojindo, Kumamoto, Japan), 3.3 nM epidermal growth factor (EGF; R&D Systems, Minneapolis, MN), 400 nM hydrocortisone (Sigma), and 870 nM zinc-free insulin (Sigma) in humidified air with 5% CO_2 at 37°C. HPMC from spent peritoneal dialysis effluent of glucose-based pH-neutral peritoneal dialysis solution were obtained by centrifugation of dialysis fluid taken randomly from the clinically stable patients with a variety of peritoneal permeability undergoing nocturnal exchanges using modified methods described previously (5, 6, 9, 26, 50, 56). HPMC were cultured under two different conditions:

1) Cellular components were isolated by low-speed (200 *g*) centrifugation, washed with RPMI 1640 (Sigma), and then cultured in RPMI 1640 containing L-glutamine (Sigma) supplemented with 15% FBS (Sigma), insulin/transferrin/selenium A (Invitrogen, Tokyo, Japan), 10^{-5} M 2-mercaptoethanol (Wako, Osaka, Japan), 3.3 nM EGF (R&D Systems) and 400 μg/l hydrocortisone (Sigma) in humidified air with 5% CO_2 at 37°C. Nonadherent material was removed the next day with two brief washes with RPMI 1640, and the adherent population was incubated in fresh culture medium. The cells reached confluence in 7–10 days, and were split two to three times and cultured. Under subconfluent conditions, HPMC and Met-5A were washed twice with PBS, and culture medium was replaced with serum-free medium for 24 h to render the cells quiescent. Subsequently, cultures were incubated with 5 ng/ml recombinant human TGF-β_1 (R&D Systems), which was diluted in serum-free medium. Cells were harvested at 0 (basal condition), 3, 6, 12, and 24 h (n = 4 dishes at each time point of each patient). All experiments were performed during 3rd to 4th passage. To explore correlation between amplification of CTGF expression by TGF-β and D/P Cr, we assessed the increase of CTGF mRNA after 12 and 24 h incubation with TGF-β_1.

2) To evaluate CTGF mRNA expression in cell culture conditions without EGF, the harvested HPMC were cultured on dishes precoated with type I collagen (Iwaki, Tokyo, Japan, cat. no. 4010-010) (n = 4 dishes of each patient). Characterization of mesothelial cells was based on both morphology and positive immunofluorescence staining with mouse anti-human cytokeratin 18 (Dako) and rabbit anti-zonula occludens (ZO)-1 (Zymed Laboratories, South San Francisco, CA) and absence of staining for CD68 (PG-M1; Dako), CD31 (JC/70A; Dako), and α-SMA (Dako).

RNA Preparation from Peritoneal Tissues and Cultured Mesothelial Cells and PCR

RNA preparation from human peritoneal tissues and cultured mesothelial cells were done using the RNeasy Fibrous Tissue Mini Kit or RNeasy Mini Kit (Qiagen) as described previously.

First-strand cDNA was synthesized by using the QuantiTect Reverse Transcription Kit (Qiagen) according to the manufacturer's instructions. A total of 1 μg of RNA was reverse transcribed. To validate gene expression changes, quantitative PCR analysis was performed with an Applied Biosystems Prism 7500HT Sequence Detection System using TaqMan Gene Expression Assays for CTGF (assay identification number Hs00170014_m1), bone morphogenic protein (BMP)-4 (Hs00370078_m1) and 18S ribosomal RNA (4319413E) according to the manufacturer's specifications (Applied Biosystems, Foster City, CA). The thermal cycler conditions were as follows: hold for 10 min at 95°C, followed by two-step PCR for 40 cycles of 95°C for 15 s and 60°C for 1 min. All reactions were performed in triplicate. Amplification data were analyzed with Ap-

plied Biosystems Sequence Detection Software version 1.3.1 (Applied Biosystems). To normalize the relative expression of the CTGF mRNA against the 18S ribosomal RNA control, standard curves were prepared in each experiment.

SDS-PAGE and Western Blotting Analyses

CTGF. CTGFs present in PD fluid samples from 2 different patients were isolated by immunoprecipitation (IP), resolved by SDS-PAGE and detected by Western blotting to determine MWs. A CTGF monoclonal antibody against *domain 1* (2 μg/ml in 1% BSA-0.05% Tween; FibroGen) was added to 0.5-ml samples of PD fluid and immune complexes were allowed to form by rotating the samples at 4°C for 30 min. Immune complexes were collected on Protein A Sepharose (Sigma, St. Louis, Mo; cat. no. P-9424) after 6 h at 4°C with rotation, washed twice with D-PBS (Ca^{2+}-, Mg^{2+}-free, Mediatech, Herndon, VA; cat. no. 21-031-CV), and eluted by use of Laemmli sample buffer without DTT or β-mercaptoethanol. Unreduced samples were heated at 70°C for 10 min and resolved by SDS-PAGE (4–12% nonreducing gradient gel, Invitrogen, Carlsbad, CA; cat. no. NP0335BOX), and proteins were transferred to nitrocellulose (8-min transfer, Invitrogen iBlot). Blots were blocked with 1% BSA-0.05% Tween 20 at 4°C overnight and total CTGF species (W-CTGF and N-CTGF) were detected by exposing the blot to a CTGF monoclonal antibody against *domain 2* (Fibro-

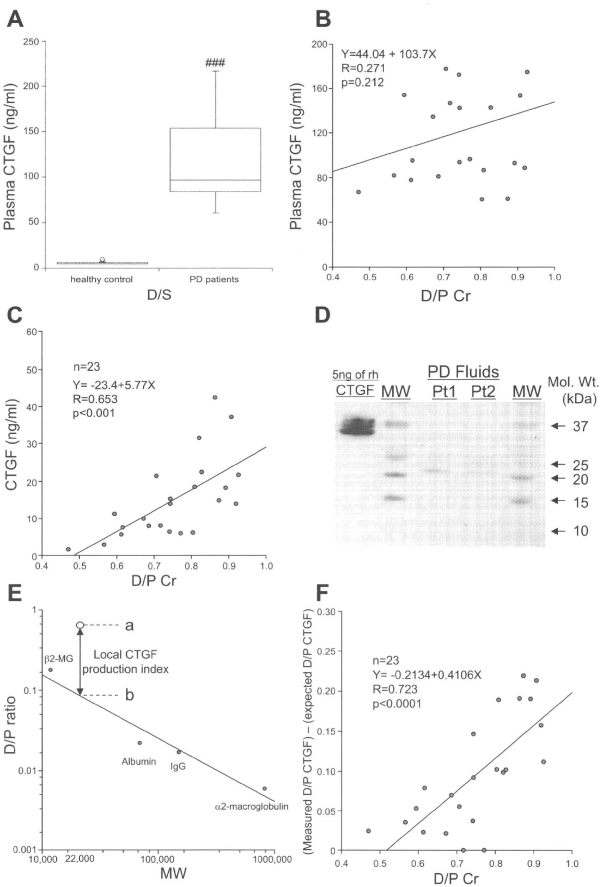

Fig. 1. Concentration of connective tissue growth factor (CTGF) in the plasma and dialysate levels in the peritoneal equilibration tests (PET). *A*: plasma CTGF levels in healthy control individuals (n = 12) and in peritoneal dialysis (PD) patients (n = 23). ###P < 0.0001. *B*: there is no relationship between plasma CTGF levels and the ratio of creatinine concentrations in dialysate and plasma (D/P Cr) at 4 h in PD patients. *C*: there is a positive correlation between CTGF concentration in the PD effluent of 4 h dwelling and peritoneal transport rate (D/P Cr). *D*: immunoprecipitation and Western blot analysis reveals CTGF reactive fragments of 22 kDa and diffuse 25–28 kDa in the spent peritoneal dialysate. Mo. Wt., molecular weight. *E*: representative case of regression line based on the power relationship between the D/P ratio of β_2-microglobulin, albumin, IgG, and α_2-macroglobulin (●) and their molecular weights (MW). The measured dialysate-to-plasma ratio of CTGF (D/P CTGF; ○, *A*) is given at the molecular weight of CTGF in the dialysate (22,000). Local peritoneal CTGF production index is calculated from the difference between measured D/P CTGF (*a*) from the regression line of each patient and expected D/P CTGF values (*b*) transported from the circulation to the peritoneal cavity. *F*: local peritoneal CTGF production index calculated from the regression line from the each patient is significantly correlated with D/P Cr.

Gen) at 2 μg/ml in 1% BSA-0.05% Tween 20 in D-PBS for 4 h at room temperature with agitation. CTGF bands were visualized by treating blots with goat anti-mouse IgG-horseradish peroxidase (1:5,000) and Pierce Luminescence reagents (Pierce, Rockford, IL) at room temperature followed by exposing blots to X-ray film. For comparison, Chinese hamster ovary (CHO) cell-derived W- and N-rhCTGFs were included on the gel, and MWs were determined by comparing mobilities of CTGF bands and MW standards (Bio-Rad Laboratories, Hercules, CA, cat. no. 161-0374).

TGF-β type II receptor. To detect TGF-β type II receptor on HPMC from six patients in the highest and lowest PET category each, we modified our previously reported technique (21). Briefly, protein amount of lysates was measured by BCA protein assay kit (Pierce). Lysates, in which protein amounts were adjusted, were mixed with sample buffer for SDS-PAGE and separated under nonreducing condition on 20% gels. Separated proteins were transferred to nitrocellulose membrane (Bio-Rad Laboratories), and membranes were blocked with 5% (wt/vol) nonfat milk in PBS (PBS-M). Membranes were then probed with a polyclonal goat anti-TGF-β type II receptor polyclonal antibody (R&D Systems) diluted in PBS-M, washed in PBS containing 0.1% Tween 20, and then probed with horseradish peroxidase-conjugated rabbit anti-goat IgG (Cappel, Durham, NC) absorbed with normal human serum (1:1 vol/vol). After they were washed again in PBS containing 0.1% Tween 20, bands were developed using enhanced chemiluminescence (GE Healthcare Bio-Sciences KK, Tokyo, Japan) and captured on LAS-300 image analysis system (FujiFilm, Tokyo, Japan).

Statistical Analysis

Values are expressed as means ± SD. Differences between groups were analyzed by Student's *t*-test or one-way ANOVA followed by Dunnett's multiple comparison tests. Correlations were assessed by the linear regression. Differences were considered to be statistically significant if $P < 0.05$. All analyses were performed using SPSS (Chicago, IL). Polynomial regression analysis was performed by using Prism 5 (GraphPad Software, La Jolla, CA).

RESULTS

CTGF Concentration in the Plasma and Peritoneal Effluent and Local Peritoneal CTGF Production in the PET

To address the possibility that CTGF content in the PD effluent could be a biomarker of peritoneal dialysis, we measured both plasma and dialysate CTGF (N-CTGF and/or W-CTGF) by sandwich ELISA. Plasma CTGF levels were significantly increased in PD patients compared with healthy controls (121.97 ± 47.36 vs. 5.76 ± 1.50 ng/ml, $P < 0.0001$, Fig. 1*A*). There was no correlation between plasma CTGF levels and the peritoneal transport rate D/P Cr in the PD patients (Fig. 1*B*). We found a positive correlation between CTGF concentration in PD effluent from 4-h dwelling times and D/P Cr, an index of peritoneal transport ($R = 0.653$, $P < 0.001$, Fig. 1*C*). For calculation of peritoneal transport of CTGF, we performed IP and Western blot analysis to determine MWs and species of CTGF in peritoneal effluent. The intact form of CTGF (36–38 kDa) was not identified, whereas CTGF reactive fragments of 22 kDa and diffuse 25–28 kDa were demonstrated (Fig. 1*D*). Most of the measured CTGF effluent dialysate concentrations (*point a* of Fig. 1*E*) were significantly greater than CTGF levels that could be expected due to simple diffusion from circulation to the dialysate using the peritoneal transport line (*point b*). The difference defines the potential extent of local peritoneal CTGF production, designated as "local CTGF production index" (Fig. 1*E*). Local CTGF production indexes correlated well with D/P Cr ($R = 0.723$, $P < 0.0001$, Fig. 1*F*). W-CTGF in the spent PD effluent was not detected by ELISA, which is consistent with IP and Western blot results.

Concentration of CTGF in the Overnight Human PD Effluent

We further assessed CTGF concentration in overnight dwelled peritoneal dialysis effluent of 155 patients and evaluated relationships with peritoneal transport rate and duration of treatment. There was a positive correlation between dialysate CTGF concentration and the D/P Cr ratio (Fig. 2*A*, $R = 0.603$), and a correlation with duration of PD treatment (Fig. 2*B*, $R = 0.264$).

CTGF mRNA Expression and Correlation With Peritoneal Thickness and the Number of Blood Vessels in Human Peritoneal Biopsy Samples

We next investigated CTGF expression in the peritoneal membrane before and after treatment with PD. Peritoneal

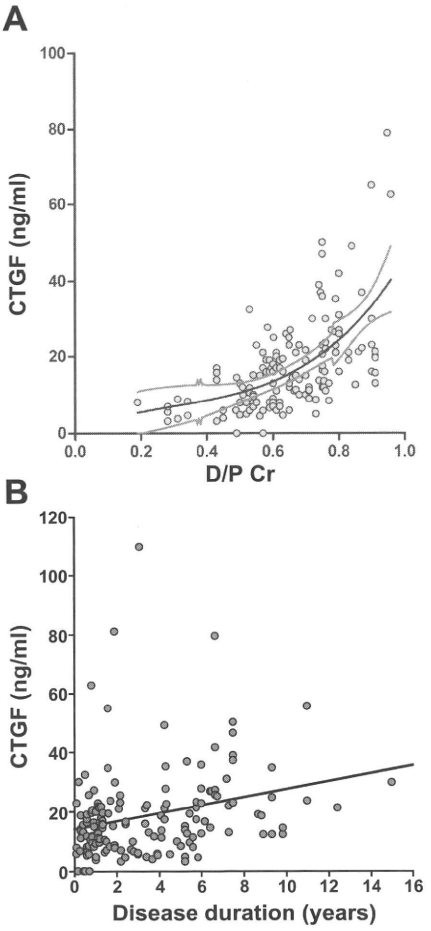

Fig. 2. Concentration of CTGF in the overnight human PD effluent. There was a positive correlation between dialysate CTGF concentration and dialysate to plasma creatinine ratio (D/P Cr) (*A*) and a correlation with duration of PD treatment (*B*). *A*: $Y = 7.377^{-0.011} + 40.84X - 83.97X^2 + 88.72X^3$, $n = 144$, $R = 0.6031$, $R^2 = 0.3637$, 95% confidence interval in gray. *B*: $Y = 14.06 + 1.347X$, $n = 155$, $R = 0.264$, $R^2 = 6.99 \times 10^{-2}$, $P < 0.001$.

membrane in the group of pre-PD renal failure (157.9 ± 17.9 μm) was thicker compared with the normal peritoneum reported by Williams et al. (49) (50 μm) and Honda et al. (17) (62.4 ± 52.0 μm). In UFF and peritonitis conditions, the peritoneum was remarkably thickened (308.6 ± 48.8 and 432.1 ± 144.4 μm, respectively). CTGF mRNA expression assessed by real-time PCR was 11.4-fold higher in peritoneal membranes with UFF vs. biopsy samples at insertion of PD catheter (pre-PD renal failure peritoneum) (Fig. 3*A*). There was a correlation between CTGF mRNA expression and thickness of submesothelial compact zone of the peritoneum in the groups of control and incidental patients ($R = 0.61$, $P < 0.0001$) and in all patients other than peritonitis ($R = 0.57$, $P < 0.0001$) (Fig. 3, *B* and *C*). However, we could not find a relationship between CTGF mRNA expression and blood vessel density of the peritoneum in either group (Fig. 3, *D* and *E*).

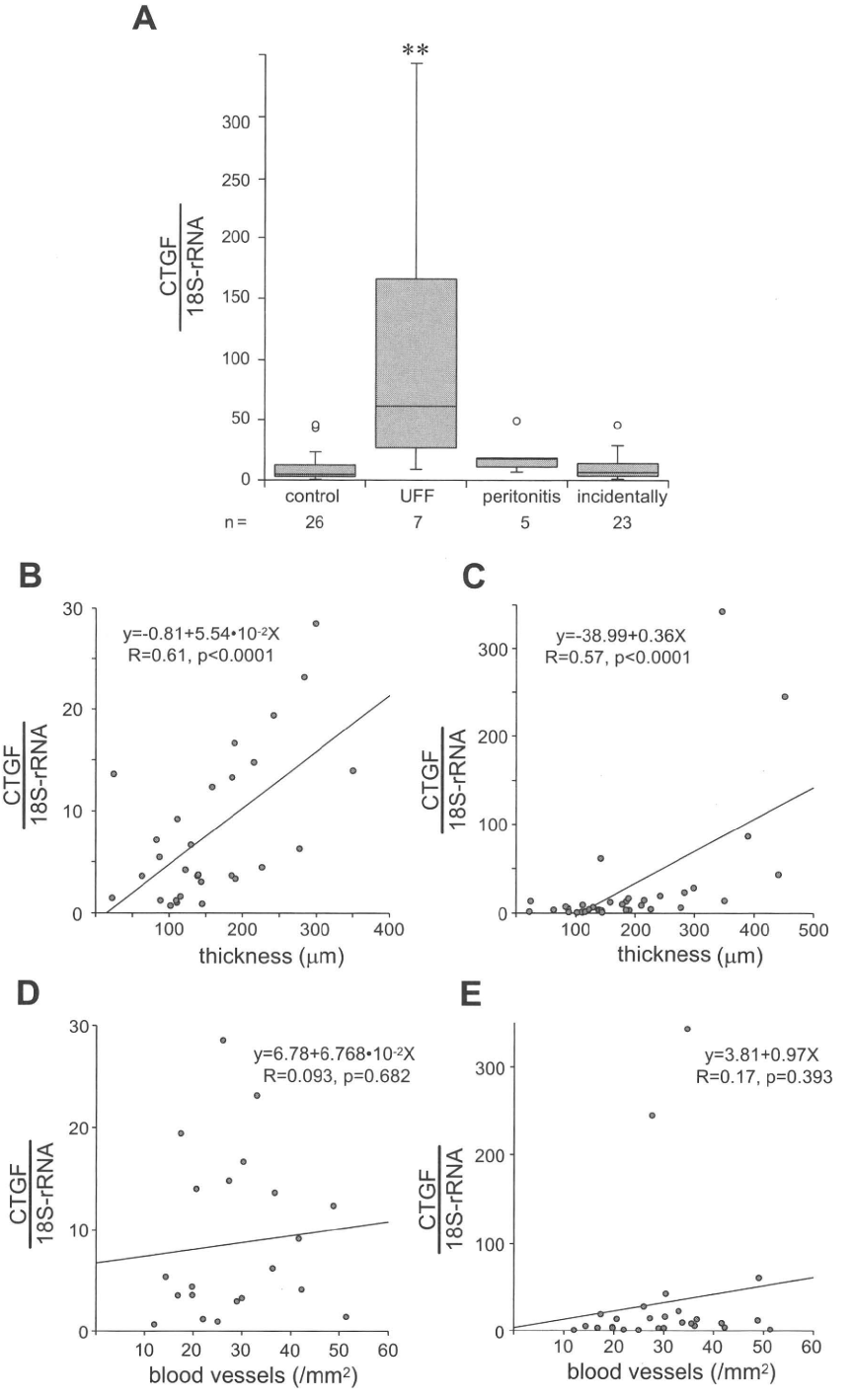

Fig. 3. CTGF mRNA expression detected by real-time PCR in human peritoneal biopsy samples and correlation with peritoneal thickness and the number of blood vessels. *A*: CTGF mRNA expression in peritoneal biopsy samples ($n = 61$) was assessed by real-time PCR. Control, peritoneal tissues were taken at the time when PD catheter was inserted because of renal failure; UFF, cases of ultrafiltration failure; incidental, peritoneal tissues were taken when the catheter was removed because of reasons other than UFF; ##$P < 0.001$ compared against controls. *B*: correlation between CTGF mRNA expression and thickness of submesothelial compact zone in the groups of control and incidental patients. *C*: correlation between CTGF mRNA expression and thickness of submesothelial compact zone in all groups other than peritonitis group. *D*: there is no correlation between CTGF mRNA expression and density of blood vessels of the peritoneum in the groups of control and incidental patients. *E*: there is no correlation between CTGF mRNA expression and density of blood vessels of the peritoneum in all groups other than peritonitis group.

Localization of CTGF mRNA and Protein Expression in the Peritoneal Tissues

ISH and IHC weakly detected CTGF mRNA and protein in the mesothelial cells and vascular wall of peritoneal tissues from patients with chronic renal failure before initiation of dialysis (Fig. 4, *A* and *B*). In the patients whose catheters were removed incidentally, CTGF was identified in the mesothelial cells and vessel walls (Fig. 4, *C* and *D*). The extent of CTGF expression was similar or slightly increased when compared with pre-PD renal failure group. In the advanced fibrotic peritoneum, mesothelial cells were partially detached from the surface of the peritoneum. However, CTGF mRNA and protein were strongly detected in the mesothelial cells and in fibroblast-like spindle-shaped cells (Fig. 4, *E* and *F*). Immunostaining for α-SMA suggested these CTGF-positive spindle-shaped cells were fibroblasts (Fig. 4*E*, *inset*).

Morphological Features and CTGF mRNA Expression in the Cultured HPMC Under Basal Condition

Human mesothelial cells (HPMC) were isolated from the spent peritoneal dialysis effluent of 32 PD patients and cultured on the collagen-I coated dish. We could not find obvious morphological differences in cells from patients of variable peritoneal transport rates (Fig. 5*A*; PET low, 5*B*; PET high). All cells appeared cobblestone shaped and were positive for ZO-1 and cytokeratin-18 but negative for α-SMA, CD68, CD31, and factor VIII by IHC analysis. In contrast, HPMC grew rapidly in culture on the noncoated dishes in the presence of EGF, adopting a spindle fibroblast-like shape as previously reported (26). We studied the CTGF mRNA content of HPMC in both culture conditions. There was no significant correlation between the rate of peritoneal membrane transport (D/P Cr) in the PD patient of origin and the basal CTGF mRNA expression under EGF-positive ($P = 0.601$) or -negative ($P = 0.452$) culture conditions with or without type I collagen. Also no correlation between basal CTGF mRNA expression and duration of PD treatment (EGF-positive condition; $P = 0.748$, EGF-negative condition; $P = 0.822$) was found. We confirmed that all of the spindle-shaped HPMC cultured in EGF-containing medium reversibly modified into the polygonal, cobblestone-shaped, epithelioid morphology after seeding and culture on collagen dishes.

CTGF mRNA Expression After Incubation With TGF-β_1 in Cultured HPMC and Met-5A Mesothelial Cell Line

The time course of CTGF mRNA expression in response to TGF-β_1 treatment was studied in both HPMC and Met-5A

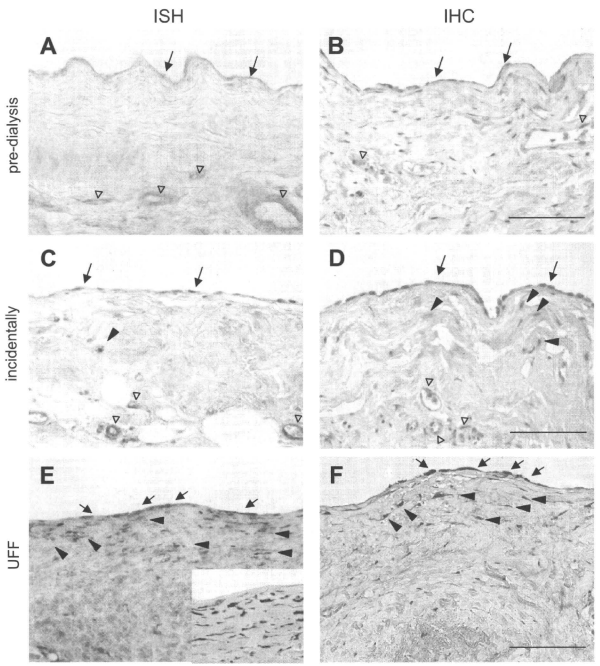

Fig. 4. CTGF mRNA and protein expression in the peritoneal tissues by in situ hybridization (ISH) and immunohistochemistry (IHC). CTGF mRNA (*A*) and protein (*B*) were weakly detected in the mesothelial cells (arrow) and vascular wall of peritoneal tissues (open arrow) from the patients with predialysis chronic renal failure. In the patients whose catheters removed incidentally (*C* and *D*), CTGF was demonstrated in the mesothelial cells (arrow) and some fibroblast-like cells (arrowhead). Open arrowheads indicate the positive expression in the vessels. In advanced fibrotic peritoneum (*E* and *F*), mesothelial cells were partly lost on the surface of the peritoneal membrane. CTGF mRNA (*E*) and protein (*F*) were strongly detected in the mesothelial cells (arrow) and fibroblast like spindle-shaped cells (arrowhead). Counterstaining was not performed on the ISH sections. Most of these spindle-shaped cells were α-smooth muscle actin (α-SMA)-positive cells (*inset*, α-SMA IHC counterstained with hematoxylin). Scale bars: 100 μm.

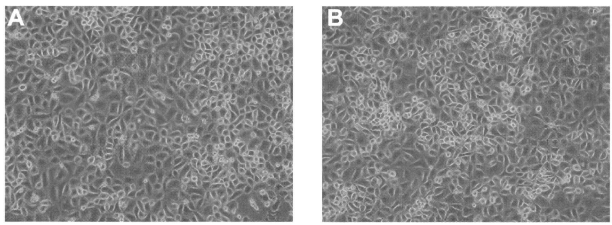

Fig. 5. Morphological differences in the cultured human peritoneal mesothelial cells (HPMC) under basal conditions. Morphological differences of mesothelial cells were not demonstrated between mesothelial cells from dialysate effluent of high permeable peritoneal function (PET high; *B*) and low permeable peritoneal function (PET low; *A*).

cells. Samples were taken after 3, 6, 12, and 24 h of exposure to TGF-β_1 (5 ng/ml). In 24 HPMC derived from 32 patients and Met-5A cells, CTGF mRNA expression was increased and peaked at 12 h. In another eight strains of HPMC CTGF mRNA expression peaked at 24 h after incubation with TGF-β_1 (Fig. 6, *A* and *B*). Therefore, we evaluated the increment of CTGF induction by TGF-β_1 at both 12 and 24 h post-TGF-β_1 exposure. Increase of CTGF mRNA at 12 h (fold) showed a good correlation with D/P Cr in both the PD patient group treated less than 2 yr with PD ($r = 0.802$, $P < 0.0001$) and all-patients group ($R = 0.668$, $P < 0.0001$, Fig. 7, *A* and *B*). This suggests that mesothelial cells from high peritoneal solute transport groups induce higher levels of CTGF by TGF-β_1. Correlation was higher at 12 h than at 24 h (Fig. 7). No significant correlation between the extent of TGF-β_1-induced increase of CTGF mRNA expression in HPMC and the duration of PD treatment of the patients from which the HPMC were derived was found (Fig. 8). Western blotting did not reveal differences in the levels of TGF-β type II receptor expression on the HPMC of patients with high peritoneal transport compared with those with low peritoneal transport, therefore excluding this as a possible factor in differential induction of CTGF expression by TGF-β in these groups of HPMC (Fig. 9).

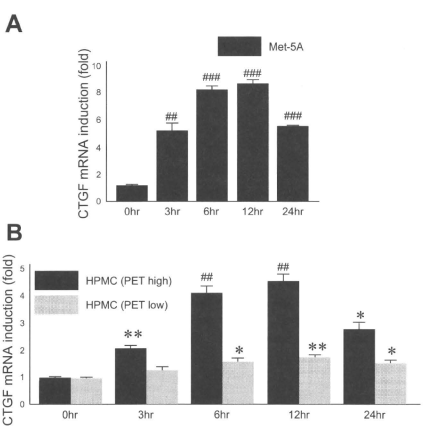

Fig. 6. CTGF mRNA expression after incubation with TGF-β_1 in Met-5A (mesothelial cell line) and HPMC. CTGF mRNA expression was studied 3, 6, 12, and 24 h post-TGF-β_1 stimulation (5 ng/ml). *A*: TGF-β_1 (5 ng/ml) stimulation on the Met-5A; $n = 4$ dishes of each time point. *B*: CTGF mRNA expression after TGF-β_1 stimulation on the HPMC from the spent PD fluid of the patient with high permeability (PET high) and with low permeability (PET low) ($n = 4$ dishes of each time point). Figures indicate 1 of the representative cases from each category. $*P < 0.05$, $**P < 0.005$, $\#\#P < 0.001$, $\#\#\#P < 0.0001$ vs. 0 h.

BMP-4 mRNA Expression Before and After Incubation With TGF-β_1 In HPMC

To characterize the BMP-4 expression after exposure to TGF-β_1, we examined the time course of BMP-4 mRNA in HPMC. TGF-β_1 induced a transient decrease of BMP-4 expression in HPMC of patients with low/low average peritoneal transport. In contrast, BMP-4 mRNA expression continued to be downregulated at 12–24 h after incubation with TGF-β_1 in HPMC from the high peritoneal transport patients. (Fig. 10*A*). We found a good inverse correlation between D/P Cr and BMP-4 mRNA levels 12 h after exposure to TGF-β_1 in both the PD patient groups treated less than 2 yr ($R = -0.678$, $P < 0.001$) and all-patients group ($R = -0.500$, $P < 0.01$), which was reciprocal to the CTGF response on TGF-β_1 exposure (Fig. 10, *B* and *C*). No correlation was observed between D/P Cr and basal BMP-4 mRNA expression both with and without presence of EGF ($P = 0.474$).

DISCUSSION

Although there is increasing evidence that peritoneal membrane failure is associated with fibrosis and neoangiogenesis, the precise mechanisms of interactions between peritoneal fibrosis and ultrafiltration failure have not been defined. Peritoneal dialysis treatment itself had a strong impact on the progression of peritoneal fibrosis/sclerosis (17), and the submesothelial compact zone thickness increased significantly with duration of PD therapy and was remarkable in the state of UFF (49). In our analysis, CTGF mRNA was significantly increased in the UFF group and was correlated with thickness of the peritoneum in all groups other than peritonitis. We excluded the cases with peritonitis in this analysis, because peritoneum can be thickened by the acute inflammatory changes with strong cell infiltration, exudation of fibrin, and edema (13a, 35). By IHC and ISH, CTGF protein and mRNA were detected in the mesothelial cells and fibroblasts in the thickened peritoneal membrane associated with high peritoneal transport. These findings indicate that CTGF is likely to be involved in peritoneal fibrosis and UFF.

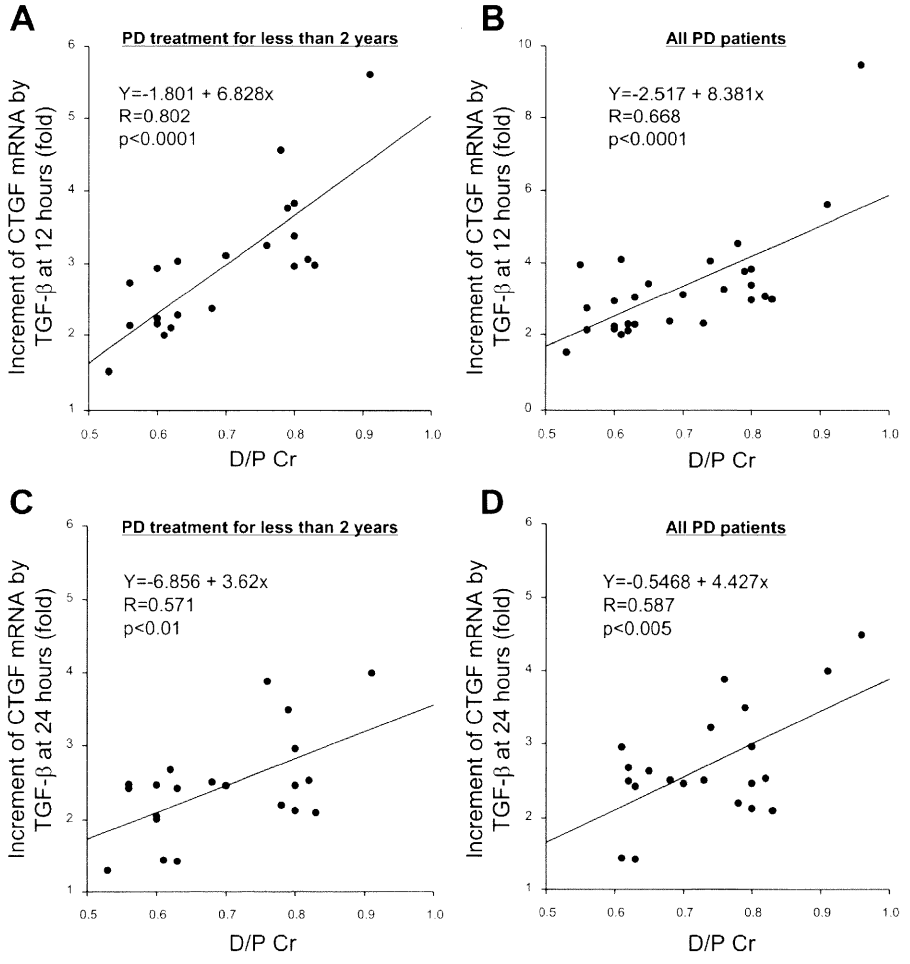

Fig. 7. Relationship between "CTGF amplification ratio" and peritoneal permeability. Relationship between peritoneal permeability (D/P Cr) and increment of CTGF mRNA expression after stimulation with TGF-β_1 in cultured mesothelial cells from the spent PD effluent. *A*: 12 h after stimulation with TGF-β_1 (5 ng/ml), treatment for less than 2 yr. *B*: 12 h after stimulation with TGF-β_1 (5 ng/ml), all patients. *C*: 24 h after stimulation with TGF-β_1 (5 ng/ml), treatment for less than 2 yr. *D*: 24 h after stimulation with TGF-β_1 (5 ng/ml), all patients.

Higher levels of plasma CTGF in PD patients may be affected by several factors, such as *1*) accumulation by reduced renal clearance; *2*) production by proliferative renal cells, preretinal tissues, blood vessel endothelial cells, and peritoneal tissues (16, 33, 34, 36); *3*) absorption of PD fluid, which contains CTGF, through lymphatic vessels (29, 42). In this respect, local peritoneal CTGF production may contribute to the high levels of plasma CTGF. CTGF in PD effluent might be derived from the circulation and/or be locally produced in the peritoneum, especially by mesothelial cells and fibroblasts, which is consistent with the ISH and IHC results. In contrast to the rapid removal of the small-molecular-weight solutes such as urea and creatinine into the PD fluid, the extent of low MW protein transfer from circulation to PD fluid is dependent on several factors including dwelling time and MW (23). Diffusion of full-length and fragmentary CTGF from circulation to PD fluid can be expected to increase linearly with time. Based on these concepts, local peritoneal production of CTGF can be calculated by the difference between the measured and expected dialysate concentration by using the peritoneal transport line determined for each patient. IP/Western blotting showed that CTGF proteins in the peritoneal effluent were 22-kDa and 25- to 28-kDa peptides, a proteolytically processed form of CTGF. Smaller fragments of CTGF can more easily diffuse from the circulation to the peritoneal fluid. Therefore, local production of CTGF using individual peritoneal transport lines was calculated at the MW 22 kDa to estimate the minimum local production rate. In addition, charge may affect the D/P ratio. β_2-Microglobulin, albumin, and α_2-macroglobulin are negatively charged, and their isoelectric points are 6.5, 6.2, and 6.4, respectively. In contrast, CTGF is positively charged with an isoelectric point of 8.0 (//www.ensembl.org/index.html) and therefore is prone to adhere to the peritoneal membrane, which is negatively charged by glycosaminoglycans and proteoglycans (14, 55). CTGF is generally considered to be a "sticky" protein and the COOH-terminal half of CTGF is known to bind heparin sulfate proteoglycans (15). A recent report has further shown that the NH_2-terminal half of CTGF can bind aggrecan (2). In this respect, the actual local CTGF production may be even higher than the calculated local production of CTGF. Another complication to consider is that after initiation of PD, the amount of glycosaminoglycans and proteoglycans may change (55). Presently it is not possible to correct for these factors in the formula of calculation. Nevertheless, our calculations indicate that local peritoneal CTGF production correlates well with peritoneal transport D/P Cr ($R = 0.723$, $P < 0.0001$), suggesting that peritoneal membranes in patients with higher peritoneal transport rates are characterized by production of larger amounts of CTGF. This is consistent with the positive correlation between D/P Cr and TGF-β-induced

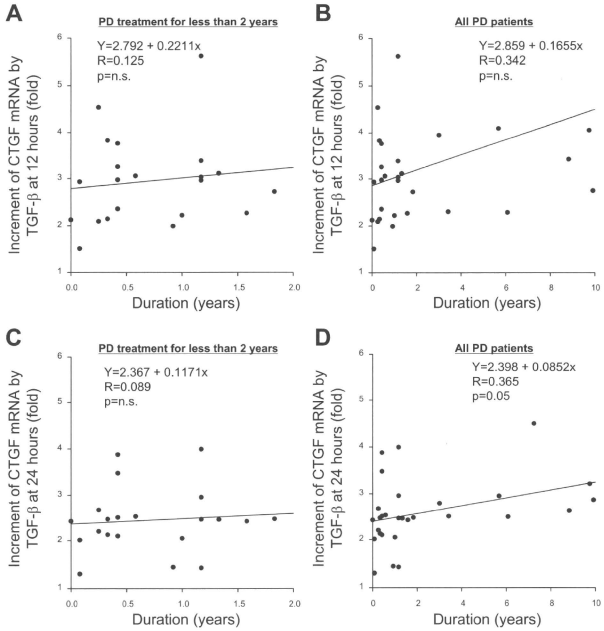

Fig. 8. Relationship between "CTGF amplification ratio" and duration of PD treatment. Relationship between duration of treatment with PD and increment of CTGF mRNA expression in cultured mesothelial cells from the spent PD effluent. *A*: 12 h after stimulation with TGF-β_1 (5 ng/ml), treatment for less than 2 yr. *B*: 12 h after stimulation with TGF-β_1 (5 ng/ml), all patients. *C*: 24 h after stimulation with TGF-β_1 (5 ng/ml), treatment for less than 2 yr. *D*: 24 h after stimulation with TGF-β_1 (5 ng/ml), all patients.

CTGF production that we observed in cultured mesothelial cells from spent effluents and strong expression of CTGF demonstrated by IHC and ISH in the UFF group. Therefore, because abnormally elevated CTGF production correlates with peritoneal fibrosis, use of CTGF as a biomarker by measuring CTGF content in PD effluent could provide important information about peritoneal transport abnormalities and activity of the peritoneal fibrotic process. TGF-β was also reported to be elevated in the PD effluent and was correlated with peritoneal transport D/P (24). There are many mechanisms including exposure to glucose, advanced glycation end products (AGE), glucose degradation products, IL-1, and angiotensin II, to upregulate TGF-β in the mesothelial cells of the PD patients (3, 27, 47). Thus high levels of both TGF-β and CTGF in PD effluent of high transport patients might strongly enhance profibrotic activity in the peritoneal cavity.

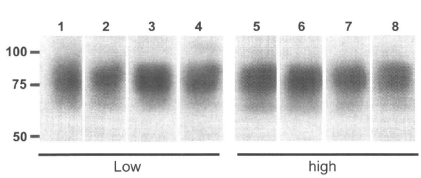

Fig. 9. Western blotting of TGF-β type II receptor on the cultured HPMC. *Lanes 1* to *4* are from different patients with the high category and *lanes 5* to *8* were from the low category of the PET. There are no differences between 2 groups. Representative cases are shown.

Mesothelial cells are the main components of peritoneum and play an important role in peritoneal homeostasis including antigen presentation, clearance of fibrin, synthesis of cytokines, growth factors, and matrix proteins (56). There are increasing data about the role of mesothelial cells in determining the functional alteration of peritoneum during PD. HPMC isolated from spent dialysate of PD patients cannot be termed "normal." Nevertheless, studies using PD-derived HPMC may provide essential data of the physiological status of renal failure and the patient's own peritoneal status during PD (56). Cells obtained from spent dialysis effluent from PD patients were reported to be enlarged and multivacuolated and to have reduced microvilli density and dysfunctional mitochondria in long-term PD therapy (8, 51, 56). Investigations into the role of mesothelial cells in the structural and functional alterations of the peritoneum during PD have shown that mesothelial cells lose epithelial phenotype and acquire myofibroblast phenotype by an EMT (3, 50). The prevalence of nonepithelioid cells by culture on the type I collagen plates in the absence of EGF conditions was reported to be related to the duration of CAPD (50). During the first 2 yr of PD, EMT of mesothelial cells is

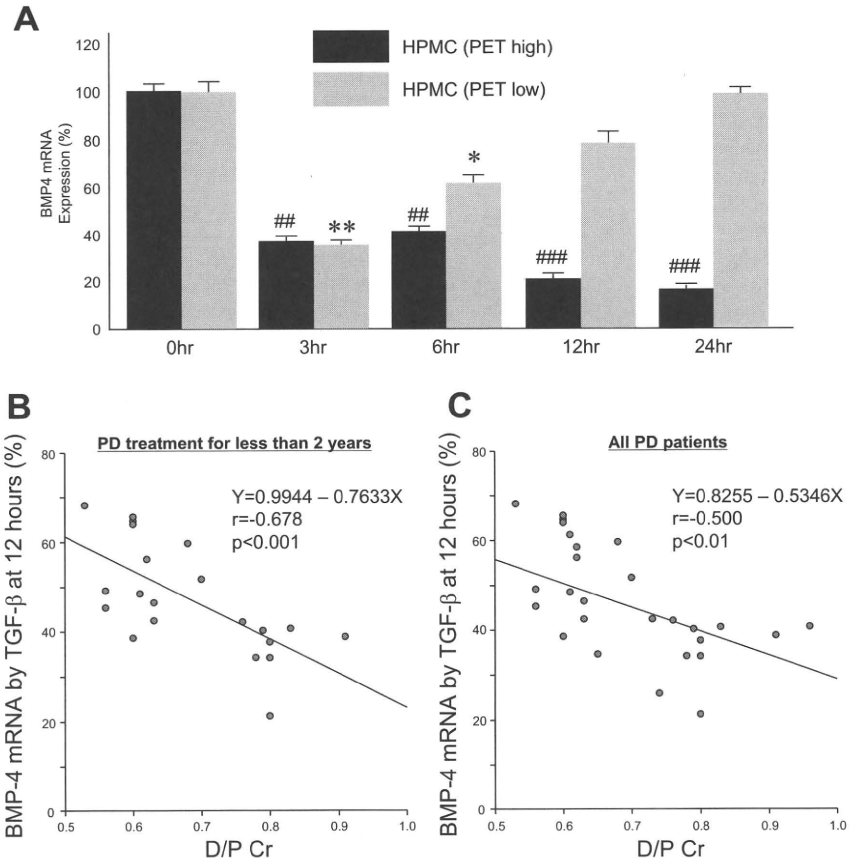

Fig. 10. BMP-4 mRNA expression after incubation with TGF-β_1 in the cultured HPMC. *A*: BMP-4 mRNA expression is downregulated from 3 to 24 h after incubation with TGF-β_1 in the PET high category patient. In contrast, BMP-4 is decreased transiently and recovered at 12 and 24 h in the PET low category patient. Representative cases are shown. $*P < 0.05$, $**P < 0.005$, $\#\#P < 0.001$, $\#\#\#P < 0.0001$ vs. 0 h. *B*: relationship between peritoneal permeability (D/P Cr) and increment of BMP-4 mRNA expression in cultured mesothelial cells from the spent PD effluent. 12 h after stimulation with TGF-β_1 (5 ng/ml), treatment for less than 2 yr. *C*: relationship between peritoneal permeability (D/P Cr) and increment of BMP-4 mRNA expression in cultured mesothelial cells from the spent PD effluent. 12 h after stimulation with TGF-β_1 (5 ng/ml), all patients.

a frequent morphological change in the peritoneal membrane (50). In addition, the prevalence of nonepithelioid cells was detected in the high transport status (13). However, in our experiments all patients' mesothelial cells from the spent dialysis fluid cultured on the type I collagen dishes showed a cobblestone-like appearance with positive staining for cytokeratin and ZO-1, which suggests that mesothelial cells in our experimental setup display a reduced fibrogenic phenotype compared with those in previous reports (50). These differences may be related to the usage of neutral pH dialysate in our patient groups. In contrast, mesothelial cells grew rapidly in culture when provided with serum, EGF, and hydrocortisone, adopting a fibroblast shape and forming parallel, multilayered arrays as reported previously (9). EGF was reported to transform cultured HPMC to fibroblast phenotype (26). When cells were split and subsequently cultured on a collagen matrix in absence of EGF, we established that these cells reverse their phenotype into polygonal, cobblestone epithelioid morphology with positive cytokeratin and ZO-1 staining. These findings suggest that EMT of mesothelial cells is reversible and may be followed by mesenchymal-to-epithelial transition under proper conditions. Therefore, we explored basal CTGF expression in both mesothelial cells cultured on the type I collagen dishes without EGF conditions and cultured on the noncoated dishes with EGF-positive conditions. In both conditions CTGF basal expression before TGF-β_1 stimulation was not different for mesothelial cells from patients with either high or low peritoneal solute transport. However, CTGF induction by TGF-β is quite different for these two groups.

CTGF mRNA is shown to be upregulated by TGF-β in the cultured mesothelial cells from spent PD effluent in our experiments as previously reported for rat (44) and human mesothelial cells derived from omentum (57). These findings are consistent with the notion that TGF-β is an important inducer of CTGF expression in mesothelial cells. An increased susceptibility to TGF-β exposure, leading to increased production of CTGF in mesothelial cells, may be related to the extent of fibrosis of the peritoneal membrane and corresponds with the observed phenotypic changes in patients with high peritoneal solute transport. Identification of the factors that regulate enhanced responsiveness to TGF-β may help to identify new strategies to prevent peritoneal fibrosis. First, we examined the expression of TGF-β type II receptor in the HPMC and found no differences between high and low peritoneal transport categories. To further characterize the difference we evaluated BMP-4 expression in HPMC. We demonstrated reciprocal expression patterns of BMP-4 and CTGF after exposure to TGF-β_1. CTGF was previously shown to bind directly to TGF-β and BMP-4 through its CR domain (i.e., *domain 2*) and regulate opposite effects. Recently BMP-4 was reported to inhibit TGF-β_2-induced expression of extracellular matrix protein and to have antagonistic effects on aldosterone signaling in the mesangial cells (1, 31, 32, 37, 58). Imbalance of TGF-β signaling leading to altered CTGF and BMP-4 expression in

the mesothelial cells may play an important role in the regulation of fibrogenic and antifibrogenic activity in the different PET category. Future studies are necessary to investigate whether overexpression of BMP-4 can compensate the dysregulation of TGF-β and CTGF signaling pathway in vitro and in vivo, which may lead to new strategies to control peritoneal transport. In addition, regulation with other antifibrogenic factors including BMP-7 and hepatocyte growth factor will have to be established in the future (46, 54).

Peritoneal neoangiogenesis is a major factor in development of peritoneal membrane failure, and local production of VEGF during PD has been proposed to play a central role in increased solute transport and ultrafiltration failure. VEGF has been shown to stimulate CTGF mRNA and protein production in bovine retinal endothelial cells and pericytes (43), and under certain circumstances CTGF also can exert angiogenic effects, as was demonstrated by the induction of neovascularization in rat corneal micropocket implants (4) and in chicken chorioallantoic membranes (41). In contrast, Inoki and colleagues (18) reported that CTGF inhibited VEGF-induced angiogenesis. In our studies, we did not observe any relation between CTGF expression and the number of vessels in the peritoneal membrane. This suggests that CTGF expression level may not be a major determinant of angiogenesis in the peritoneal membrane.

In summary, we report that high peritoneal transport state correlates with increased peritoneal CTGF expression and higher CTGF expression in response to TGF-β in mesothelial cells. CTGF content in spent dialysate might be a biomarker for development of peritoneal fibrosis in PD patients. Functional alteration of mesothelial cells, as exemplified by the altered balance of CTGF and BMP-4 expression induced by TGF-β, may be involved in progression of peritoneal fibrosis in the high transport state. Phenotypic control of the mesothelial cells could be a potential therapeutic target of peritoneal fibrosis and membrane failure.

ACKNOWLEDGMENTS

The technical assistance of Norihiko Suzuki, Keiko Higashide, Naoko Asano, and Yuriko Sawa (Department of Nephrology, Nagoya University, Nagoya, Japan) is gratefully acknowledged. We thank Dongxia Li, Dan Yi, Thomas Crowley, and Jay Leone (FibroGen) for the technical assistance on the ELISA and Western blotting analysis.

GRANTS

This work was supported by in part by a grant-in-aid for Scientific Research from the Ministry Education, Science, and Culture, Japan (no. 20590972), the 2007 research grant from the Aichi Kidney Foundation and Baxter Japan PD Grant 2009.

DISCLOSURES

N. Oliver is an employee of FibroGen, Inc. (San Francisco, CA), supplier of anti-CTGF antibodies; R. Goldschmeding has received research support grants and is currently also an employee of FibroGen, Inc.

REFERENCES

1. **Abreu JG, Ketpura NI, Reversade B, De Robertis EM.** Connective-tissue growth factor (CTGF) modulates cell signalling by BMP and TGF-beta. *Nat Cell Biol* 4: 599–604, 2002.
2. **Aoyama E, Hattori T, Hoshijima M, Araki D, Nishida T, Kubota S, Takigawa M.** N-terminal domains of CCN family 2/connective tissue growth factor bind to aggrecan. *Biochem J* 420: 413–420, 2009.
3. **Aroeira LS, Aguilera A, Sanchez-Tomero JA, Bajo MA, del Peso G, Jimenez-Heffernan JA, Selgas R, Lopez-Cabrera M.** Epithelial to mesenchymal transition and peritoneal membrane failure in peritoneal dialysis patients: pathologic significance and potential therapeutic interventions. *J Am Soc Nephrol* 18: 2004–2013, 2007.
4. **Babic AM, Chen CC, Lau LF.** Fisp12/mouse connective tissue growth factor mediates endothelial cell adhesion and migration through integrin alphavbeta3, promotes endothelial cell survival, and induces angiogenesis in vivo. *Mol Cell Biol* 19: 2958–2966, 1999.
5. **Betjes MG, Bos HJ, Krediet RT, Arisz L.** The mesothelial cells in CAPD effluent and their relation to peritonitis incidence. *Perit Dial Int* 11: 22–26, 1991.
6. **Bot J, Whitaker D, Vivian J, Lake R, Yao V, McCauley R.** Culturing mouse peritoneal mesothelial cells. *Pathol Res Pract* 199: 341–344, 2003.
7. **Burns WC, Twigg SM, Forbes JM, Pete J, Tikellis C, Thallas-Bonke V, Thomas MC, Cooper ME, Kantharidis P.** Connective tissue growth factor plays an important role in advanced glycation end product-induced tubular epithelial-to-mesenchymal transition: implications for diabetic renal disease. *J Am Soc Nephrol* 17: 2484–2494, 2006.
8. **Chan TM, Leung JK, Sun Y, Lai KN, Tsang RC, Yung S.** Different effects of amino acid-based and glucose-based dialysate from peritoneal dialysis patients on mesothelial cell ultrastructure and function. *Nephrol Dial Transplant* 18: 1086–1094, 2003.
9. **Connell ND, Rheinwald JG.** Regulation of the cytoskeleton in mesothelial cells: reversible loss of keratin and increase in vimentin during rapid growth in culture. *Cell* 34: 245–253, 1983.
10. **Davies SJ.** Longitudinal relationship between solute transport and ultrafiltration capacity in peritoneal dialysis patients. *Kidney Int* 66: 2437–2445, 2004.
11. **Davies SJ, Bryan J, Phillips L, Russell GI.** Longitudinal changes in peritoneal kinetics: the effects of peritoneal dialysis and peritonitis. *Nephrol Dial Transplant* 11: 498–506, 1996.
12. **Del Peso G, Fernández-Reyes MJ, Hevia C, Bajo MA, Castro MJ, Cirugeda A, Sánchez-Tomero JA, Selgas R.** Factors influencing peritoneal transport parameters during the first year on peritoneal dialysis: peritonitis is the main factor. *Nephrol Dial Transplant* 20: 1201–1206, 2005.
13. **Del Peso G, Jiménez-Heffernan JA, Bajo MA, Aroeira LS, Aguilera A, Fernández-Perpén A, Cirugeda A, Castro MJ, de Gracia R, Sánchez-Villanueva R, Sánchez-Tomero JA, López-Cabrera M, Selgas R.** Epithelial-to-mesenchymal transition of mesothelial cells is an early event during peritoneal dialysis and is associated with high peritoneal transport. *Kidney Int Suppl* 73: S26–S33, 2008.
13a. **Di Paolo N, Sacchi G.** Atlas of peritoneal histology. *Perit Dial Int* 20: S5–S96, 2000.
14. **Flessner MF.** The transport barrier in intraperitoneal therapy. *Am J Physiol Renal Physiol* 288: F433–F442, 2005.
15. **Gao R, Brigstock DR.** Connective tissue growth factor (CCN2) induces adhesion of rat activated hepatic stellate cells by binding of its C-terminal domain to integrin alpha(v)beta(3) and heparan sulfate proteoglycan. *J Biol Chem* 279: 8848–8855, 2004.
16. **Hinton DR, Spee C, He S, Weitz S, Usinger W, LaBree L, Oliver N, Lim JI.** Accumulation of NH_2-terminal fragment of connective tissue growth factor in the vitreous of patients with proliferative diabetic retinopathy. *Diabetes Care* 27: 758–764, 2004.
17. **Honda K, Hamada C, Nakayama M, Miyazaki M, Sherif AM, Harada T, Hirano H, Peritoneal Biopsy Study Group of the Japanese Society for Peritoneal Dialysis.** Impact of uremia, diabetes, and peritoneal dialysis itself on the pathogenesis of peritoneal sclerosis: a quantitative study of peritoneal membrane morphology. *Clin J Am Soc Nephrol* 3: 720–728, 2008.
18. **Inoki I, Shiomi T, Hashimoto G, Enomoto H, Nakamura H, Makino K, Ikeda E, Takata S, Kobayashi K, Okada Y.** Connective tissue growth factor binds vascular endothelial growth factor (VEGF) and inhibits VEGF-induced angiogenesis. *FASEB J* 16: 219–221, 2002.
19. **Ito Y, Aten J, Bende RJ, Oemar BS, Rabelink TJ, Weening JJ, Goldschmeding R.** Expression of connective tissue growth factor in human renal fibrosis. *Kidney Int* 53: 853–861, 1998.
20. **Ito Y, Goldschmeding R, Bende R, Claessen N, Chand M, Kleij L, Rabelink T, Weening JJ, Aten J.** Kinetics of connective tissue growth factor expression during experimental proliferative glomerulonephritis. *J Am Soc Nephrol* 12: 472–484, 2001.
21. **Kasuga H, Ito Y, Sakamoto S, Kawachi H, Shimizu F, Yuzawa Y, Matsuo S.** Effects of anti-TGF-b type II receptor antibody on experimental glomerulonephritis. *Kidney Int* 60: 1745–1755, 2001.
22. **Kawaguchi Y, Ishizaki T, Imada A, Oohhira S, Nakamoto H, Hiramatsu M, Maeda K, Ota K.** Searching for the reasons for drop-out from

peritoneal dialysis: a nationwide survey in Japan. *Perit Dial Int* 23: S175–S177, 2003.
23. **Kim DJ, Do JH, Huh W, Kim YG, Oh HY.** Dissociation between clearances of small and middle molecules in incremental peritoneal dialysis. *Perit Dial Int* 21: 462–466, 2001.
24. **Lai KN, Lai KB, Szeto CC, Lam CW, Leung JC.** Growth factors in continuous ambulatory peritoneal dialysis effluent. Their relation with peritoneal transport of small solutes. *Am J Nephrol* 19: 416–422, 1999.
25. **Leask A, Abraham DJ.** TGF-β signaling and the fibrotic response. *FASEB J* 18: 816–827, 2004.
26. **Leavesley DI, Stanley JM, Faull RJ.** Epidermal growth factor modifies the expression and function of extracellular matrix adhesion receptors expressed by peritoneal mesothelial cells from patients on CAPD. *Nephrol Dial Transplant* 14: 1208–1216, 1999.
27. **Leung JCK, Chan LYY, Li FFK, Tang SCW, Chan KW, Chan TM, Lam MF, Wieslander A, Lai KN.** Glucose degradation products down-regulate ZO-1 expression in human peritoneal mesothelial cells: the role of VEGF. *Nephrol Dial Transplant* 20: 1336–1349, 2005.
28. **Mateijsen MA, Van der Wal AC, Hendriks PM, Zweers MM, Mulder J, Struijk DG, Krediet RT.** Vascular and interstitial changes in the peritoneum of CAPD patients with peritoneal sclerosis. *Perit Dial Int* 19: 517–525, 1999.
29. **Michels WM, Zweers MM, Smit W, Korevaar J, Struijk DG, van Westrhenen R, Krediet RT.** Does lymphatic absorption change with the duration of peritoneal dialysis? *Perit Dial Int* 24: 347–352, 2004.
30. **Munemasa S, Sakai A, Kuroda Y, Okikawa Y, Katayama Y, Asaoku H, Kubo T, Miyakawa Y, Serikawa M, Sasaki T, Kimura A.** Connective tissue growth factor is an indicator of bone involvement in multiple myeloma, but matrix metalloproteinase-9 is not. *Br J Haematol* 139: 41–50, 2007.
31. **Nguyen TQ, Goldschmeding R.** Bone morphogenetic protein-7 and connective tissue growth factor: novel targets for treatment of renal fibrosis? *Pharm Res* 25: 2416–2426, 2008.
32. **Nguyen TQ, Roestenberg P, van Nieuwenhoven FA, Bovenschen N, Li Z, Xu L, Oliver N, Aten J, Joles JA, Vial C, Brandan E, Lyons KM, Goldschmeding R.** CTGF inhibits BMP-7 signaling in diabetic nephropathy. *J Am Soc Nephrol* 19: 2098–2107, 2008.
33. **Nguyen TQ, Tarnow L, Andersen S, Hovind P, Parving HH, Goldschmeding R, van Nieuwenhoven FA.** Urinary connective tissue growth factor excretion correlates with clinical markers of renal disease in a large population of type 1 diabetic patients with diabetic nephropathy. *Diabetes Care* 29: 83–88, 2006.
34. **Nguyen TQ, Tarnow L, Jorsal A, Oliver N, Roestenberg P, Ito Y, Parving HH, Rossing P, van Nieuwenhoven FA, Goldschmeding R.** Plasma connective tissue growth factor is an independent predictor of end-stage renal disease and mortality in type 1 diabetic nephropathy. *Diabetes Care* 31: 1177–1182, 2008.
35. **Nishimura H, Ito Y, Mizuno M, Tanaka A, Morita Y, Maruyama S, Yuzawa Y, Matsuo S.** Mineralocorticoid receptor blockade ameliorates peritoneal fibrosis in new rat peritonitis model. *Am J Physiol Renal Physiol* 294: F1084–F1093, 2008.
36. **Oemar BS, Werner A, Garnier JM, Do DD, Godoy N, Nauck M, März W, Rupp J, Pech M, Lüscher TF.** Human connective tissue growth factor is expressed in advanced atherosclerotic lesions. *Circulation* 95: 831–839, 1997.
37. **Otani H, Otsuka F, Inagaki K, Takeda M, Miyoshi T, Suzuki J, Mukai T, Ogura T, Makino H.** Antagonistic effects of bone morphogenetic protein-4 and -7 on renal mesangial cell proliferation induced by aldosterone through MAPK activation. *Am J Physiol Renal Physiol* 292: F1513–F1525, 2007.
39. **Perbal B.** CCN proteins: multifunctional signalling regulators. *Lancet* 363: 62–64, 2004.
40. **Selgas R, Fernandez-Reyes MJ, Bosque E, Bajo MA, Borrego F, Jimenez C, Del Peso G, De Alvaro F.** Functional longevity of the human peritoneum: how long is continuous peritoneal dialysis possible? Results of a prospective medium long-term study. *Am J Kidney Dis* 23: 64–73, 1994.
41. **Shimo T, Nakanishi T, Nishida T, Asano M, Kanyama M, Kuboki T, Tamatani T, Tezuka K, Takemura M, Matsumura T, Takigawa M.** Connective tissue growth factor induces the proliferation, migration, and tube formation of vascular endothelial cells in vitro, and angiogenesis in vivo. *J Biochem (Tokyo)* 126: 137–145, 1999.
42. **Struijk DG, Krediet RT, Koomen GC, Boeschoten EW, vd Reijden HJ, Arisz L.** Indirect measurement of lymphatic absorption with inulin in continuous ambulatory peritoneal dialysis (CAPD) patients. *Perit Dial Int* 10: 141–145, 1990.
43. **Suzuma K, Naruse K, Suzuma I, Takahara N, Ueki K, Aiello LP, King GL.** Vascular endothelial growth factor induces expression of connective tissue growth factor via KDR, Flt1, and phosphatidylinositol 3-kinase-Akt-dependent pathways in retinal vascular cells. *J Biol Chem* 275: 40725–40731, 2000.
44. **Szeto CC, Lai KB, Chow KM, Szeto CY, Wong TY, Li PK.** Differential effects of transforming growth factor-beta on the synthesis of connective tissue growth factor and vascular endothelial growth factor by peritoneal mesothelial cell. *Nephron Exp Nephrol* 99: e95–e104, 2005.
45. **Twardowski ZJ.** The fast peritoneal equilibration test. *Semin Dial* 3: 141–142, 1990.
46. **Vargha R, Endemann M, Kratochwill K, Riesenhuber A, Wick N, Krachler AM, Malaga-Dieguez L, Aufricht C.** Ex vivo reversal of in vivo transdifferentiation in mesothelial cells grown from peritoneal dialysate effluents. *Nephrol Dial Transplant* 21: 2943–2947, 2006.
47. **Vriese ASD, Flyvbjerg A, Mortier S, Tilton RG, Lameire NH.** Inhibition of the interaction of AGE-RAGE prevents hyperglycemia-induced fibrosis of the peritoneal membrane. *J Am Soc Nephrol* 14: 2109–2118, 2003.
48. **Williams JD, Topley N, Craig KJ, Mackenzie RK, Pischetsrieder M, Lage C, Passlick-Deetjen J.** The Euro-Balance Trial: the effect of a new biocompatible peritoneal dialysis fluid (balance) on the peritoneal membrane. *Kidney Int* 66: 408–418, 2004.
49. **Williams JD, Craig KJ, Topley N, Von Ruhland C, Fallon M, Newman GR, Mackenzie RK, Williams GT.** Morphologic changes in the peritoneal membrane of patients with renal disease. *J Am Soc Nephrol* 13: 470–479, 2002.
50. **YÁñez-Mó M, Lara-Pezzi E, Selgas R, Ramírez-Huesca M, Domínguez-Jiménez C, Jiménez-Heffernan JA, Aguilera A, Sánchez-Tomero JA, Bajo MA, Álvarez V, Castro MA, del Peso G, Cirujeda A, Gamallo C, Sánchez-Madrid F, López-Cabrera M.** Peritoneal dialysis and epithelial-to-mesenchymal transition of mesothelial cells. *N Engl J Med* 348: 403–413, 2003.
51. **Yamamoto T, Izumotani T, Otoshi T, Kim M.** Morphological studies of mesothelial cells in CAPD effluent and their clinical significance. *Am J Kidney Dis* 32: 946–952, 1998.
52. **Yokoi H, Mukoyama M, Mori K, Kasahara M, Suganami T, Sawai K, Yoshioka T, Saito Y, Ogawa Y, Kuwabara T, Sugawara A, Nakao K.** Overexpression of connective tissue growth factor in podocytes worsens diabetic nephropathy in mice. *Kidney Int* 73: 446–455, 2008.
53. **Yokoi H, Mukoyama M, Nagae T, Mori K, Suganami T, Sawai K, Yoshioka T, Koshikawa M, Nishida T, Takigawa M, Sugawara A, Nakao K.** Reduction in connective tissue growth factor by antisense treatment ameliorates renal tubulointerstitial fibrosis. *J Am Soc Nephrol* 15: 1430–1440, 2004.
54. **Yu MA, Shin KS, Kim JH, Kim YI, Chung SS, Park SH, Kim YL, Kang DH.** HGF and BMP-7 ameliorate high glucose-induced epithelial-to-mesenchymal transition of peritoneal mesothelium. *J Am Soc Nephrol* 20: 567–581, 2009.
55. **Yung S, Chan TM.** Glycosaminoglycans and proteoglycans: overlooked entities? *Perit Dial Int* 27: S104–109, 2007.
56. **Yung S, Li FK, Chan TM.** Peritoneal mesothelial cell culture and biology. *Perit Dial Int* 26: 162–173, 2006.
57. **Zarrinkalam KH, Stanley JM, Gray J, Oliver N, Faull RJ.** Connective tissue growth factor and its regulation in the peritoneal cavity of peritoneal dialysis patients. *Kidney Int* 64: 331–338, 2003.
58. **Zode GS, Clark AF, Wordinger RJ.** Bone morphogenetic protein 4 inhibits TGF-beta2 stimulation of extracellular matrix proteins in optic nerve head cells: role of gremlin in ECM modulation. *Glia* 57: 755–766, 2009.
59. **Zweers MM, de Waart DR, Smit W, Struijk DG, Krediet RT.** Growth factors VEGF and TGF-b1 in peritoneal dialysis. *J Lab Clin Med* 134: 124–132, 1999.
60. **Zweers MM, Struijk DG, Smit W, Krediet RT.** Vascular endothelial growth factor in peritoneal dialysis: a longitudinal follow-up. *J Lab Clin Med* 137: 125–132, 2001.

Expression patterns of connective tissue growth factor and of TGF- β isoforms during glomerular injury recapitulate glomerulogenesis

Yasuhiko Ito, Roel Goldschmeding, Hirotake Kasuga, Nike Claessen, Masahiro Nakayama, Yukio Yuzawa, Akiho Sawai, Seiichi Matsuo, Jan J. Weening and Jan Aten

Am J Physiol Renal Physiol 299:F545-F558, 2010. First published 24 June 2010;
doi:10.1152/ajprenal.00120.2009

Am J Physiol Renal Physiol 299: F545–F558, 2010.
First published June 24, 2010; doi:10.1152/ajprenal.00120.2009.

Expression patterns of connective tissue growth factor and of TGF-β isoforms during glomerular injury recapitulate glomerulogenesis

Yasuhiko Ito,[1,2] Roel Goldschmeding,[3] Hirotake Kasuga,[4] Nike Claessen,[1] Masahiro Nakayama,[5] Yukio Yuzawa,[2] Akiho Sawai,[2] Seiichi Matsuo,[2] Jan J. Weening,[1] and Jan Aten[1]

[1]*Department of Pathology, Academic Medical Center, University of Amsterdam, Amsterdam, The Netherlands;* [2]*Department of Nephrology, Nagoya University, Nagoya, Japan;* [3]*Department of Pathology, University Medical Centre Utrecht, Utrecht, The Netherlands;* [4]*Department of Internal Medicine, Nagoya Kyoritsu Hospital, Nagoya; and* [5]*Department of Clinical Laboratory Medicine and Anatomic Pathology, Osaka Medical Center and Research Institute for Maternal and Child Health, Osaka, Japan*

Submitted 1 March 2009; accepted in final form 22 June 2010

Ito Y, Goldschmeding R, Kasuga H, Claessen N, Nakayama M, Yuzawa Y, Sawai A, Matsuo S, Weening JJ, Aten J. Expression patterns of connective tissue growth factor and of TGF-β isoforms during glomerular injury recapitulate glomerulogenesis. *Am J Physiol Renal Physiol* 299: F545–F558, 2010. First published June 24, 2010; doi:10.1152/ajprenal.00120.2009.—Transforming growth factor (TGF)-β_1, -β_2, and -β_3 are involved in control of wound repair and development of fibrosis. Connective tissue growth factor (CTGF) expression is stimulated by all TGF-β isoforms and is abundant in glomerulosclerosis and other fibrotic disorders. CTGF is hypothesized to mediate profibrotic effects of TGF-β_1 or to facilitate interaction of TGF-β_1 with its receptor, but its interactions with TGF-β isoforms in nonpathological conditions are unexplored so far. Tissue repair and remodeling may recapitulate gene transcription at play in organogenesis. To further delineate the relationship between CTGF and TGF-β, we compared expression patterns of CTGF and TGF-β isoforms in rat and human glomerulogenesis and in various human glomerulopathies. CTGF mRNA was present in the immediate precursors of glomerular visceral and parietal epithelial cells in the comma- and S-shaped stages, but not in earlier stages of nephron development. During the capillary loop and maturing glomerular stages and simultaneous with the presence of TGF-β_1, -β_2, and -β_3 protein, CTGF mRNA expression was maximal and present only in differentiating glomerular epithelial cells. CTGF protein was also present on precursors of mesangium and glomerular endothelium, suggesting possible paracrine interaction. Concomitant with the presence of TGF-β_2 and -β_3 protein, and in the absence of TGF-β_1, CTGF mRNA and protein expression was restricted to podocytes in normal adult glomeruli. However, TGF-β_1 and CTGF were again coexpressed, often with TGF-β_2 and -β_3, in particular in podocytes in proliferative glomerulonephritis and also in mesangial cells in diabetic nephropathy and IgA nephropathy (IgA NP). Coordinated expression of TGF-β isoforms and of CTGF may be involved in normal glomerulogenesis and possibly in maintenance of glomerular structure and function at adult age. Prolonged overexpression of TGF-β_1 and CTGF is associated with development of severe glomerulonephritis and glomerulosclerosis.

CCN2; development; glomerulosclerosis; podocyte

CONNECTIVE TISSUE GROWTH FACTOR (CTGF or CCN2) is a member of the CCN family of structurally related proteins (11, 14, 21). The CCN proteins contain an NH_2-terminal secretory signal peptide and four structural domains: an insulin-like growth factor binding domain (*domain 1*); a chordin-like, cysteine-rich domain with similarity to von Willebrand factor type C domain (*domain 2*), which is connected via a protease-sensitive hinge region to a thrombospondin type 1 repeat (*domain 3*); and finally a COOH-terminal cystine knot (*domain 4*) (1, 11). CCN proteins are involved in regulation of essential cell functions as adhesion, migration, mitogenesis, differentiation, and survival (13, 29). As such, CCN family members have been implicated among others in control of wound repair, development of fibrosis, and tumorigenesis (20, 30, 44). CTGF, in particular, has been reported to be overexpressed in fibrosis of diverse organs (22, 34, 40, 42). Our laboratory demonstrated that CTGF mRNA is strongly upregulated in human renal fibrosis and in rat experimental proliferative glomerulonephritis (23, 24).

Transforming growth factor (TGF)-β is a key component in control of wound repair and in development of fibrosis (7, 10). CTGF mRNA expression was observed to be associated with differential expression of the three closely related isoforms of TGF-β in the course of the anti-Thy-1.1 glomerulonephritis model (24). All three TGF-β isoforms are equally able to induce upregulation of CTGF mRNA in both cultured mesangial cells and glomerular visceral epithelial cells (GVECs) (24). In vitro effects of TGF-β_1 on matrix synthesis by fibroblasts and mesangial cells do, at least partially, require the presence of CTGF (9, 30, 67). These findings suggest that CTGF may be involved in tissue repair in response to glomerular injury, possibly downstream of TGF-β. Tissue repair may recapitulate developmental programs at play in organogenesis, and comparison of these processes may yield insight in the nature of common regulatory factors. In development of the kidney in mammals, the ureteric bud is induced by the metanephric blastema to develop from the mesonephric duct. Growth of the ureteric duct comprises both elongation of the duct and (asymmetric) branching. In turn, the metanephric blastema is induced by the invading ureter branch tips to undergo nephrogenesis involving mesenchymal cell condensation and transition into polarized epithelium forming a vesicle. The vesicle undergoes patterning to form subsequently comma-shaped and S-shaped bodies. Capillary sprouts, as well as vasculogenic precursors of endothelial cells, are recruited into the cleft that is formed by the proximal curvature of the S-shaped body. The proximal and distal parts of the S-shaped body differentiate into the glomerular epithelium and into the proximal and distal tubular epithelium, respectively.

Glomerulogenesis proceeds through the capillary loop stage and the maturing stage to the adult stage, during which mesangial progenitor cells migrate into the glomerulus, the glo-

Address for reprint requests and other correspondence: J. Aten, Dept. of Pathology, Academic Medical Center, Univ. of Amsterdam, Meibergdreef 9, M2-132, 1105 AZ Amsterdam, The Netherlands (e-mail: j.aten@amc.uva.nl).

merular capillary network is shaped, and the podocytes fully differentiate. The tips of the distal tubule and the ureteric duct fuse, and further growth and transformation within the tubular compartment leads to formation of Henle's loop (50, 51).

In early stages of metanephric development in mice, the three TGF-β isoforms are expressed by the branching ureteric duct epithelium, and TGF-β_2 localization is restricted to the basal side of a subset of these epithelial cells (43). During further ramification, expression of all TGF-β isoforms decreases in the tubular epithelium and becomes apparent in the surrounding mesenchyme (43). By in situ hybridization (ISH), TGF-β_1 mRNA was found in the developing ureteric duct epithelium, as well as in mesenchymal cells in the nephrogenic zone (17). In addition, TGF-β_1 mRNA was reported to be present in early nephron structures, including condensates, comma-shaped bodies, S-shaped bodies, and immature glomeruli. In subsequent stages of nephron development, TGF-β_1 mRNA was observed in the distal part of the nephron tubules, but not in maturing glomeruli or proximal tubules (17). No detailed information on expression of TGF-β_2 or TGF-β_3 in developing glomeruli has been reported so far.

Mice that are completely deficient in TGF-β_1 (31) or lack expression of the TGF-β type II receptor (41) die at midgestation due to defects in vasculogenesis and hematopoiesis, thereby precluding information on the possible role of TGF-β_1 in nephrogenesis. In developing rat metanephroi in vitro, addition of TGF-β_1 was found to inhibit ureteric duct growth and thereby nephron endowment (17, 48). TGF-β_1 does not appear to inhibit epithelial patterning in nephron development significantly, once the epithelial vesicle is formed in these cultures (17). In contrast, neutralizing anti-TGF-β_1 does inhibit formation of the glomerular capillary network when injected in rats between *days 3* and *5* after birth (32). In metanephric explant cultures, TGF-β_2 was shown to be secreted by ureteric bud epithelial cells and to stimulate at low concentrations nephrogenesis, in cooperation with leukemia inhibitory factor and fibroblast growth factor-2 (45). In this experimental setup, TGF-β_1 and TGF-β_3 were also shown to have nephrogenic capacity (45). TGF-$\beta_2^{-/-}$ mice display varying renal phenotypes, ranging from complete renal agenesis to a dilated pelvis (49). Absence of the ureteric bud-derived TGF-β_2 is associated with strongly decreased numbers of branch tips, as well as of glomeruli in cultures of renal explants, possibly due to the loss of TGF-β_2-dependent functional mesenchyme as an active inducer of branching morphogenesis (56). Interestingly, accelerated ureteric branching morphogenesis and an associated increase in nephron number were observed in kidneys of TGF-$\beta_2^{+/-}$ mice by Sims-Lucas and colleagues (56). Apparently, when TGF-β_2 is present at reduced levels, the metanephric mesenchyme can survive and induce branching, but the previously described TGF-β_2-dependent negative feedback regulation of branching morphogenesis is alleviated (18, 56). The mean glomerular volumes were smaller in TGF-$\beta_2^{+/-}$ mice, but renal histopathology was otherwise not observed (56). CTGF has been detected in the kidney during murine embryogenesis (27, 57), but CTGF expression during glomerulogenesis has not been reported so far.

Since the TGF-β isoforms may be involved not only in early metanephric development, but also in glomerulogenesis, and, since they are potent inducers of CTGF expression in wound repair and in development of fibrosis, we investigated CTGF expression in glomerulogenesis in relation to the expression of TGF-β_1, TGF-β_2, and TGF-β_3. In addition, expression of these factors was compared in various adult human glomerulopathies with distinct patterns of injury, proliferation, and remodeling.

MATERIALS AND METHODS

Rat kidney specimens. Ten-week-old female Wistar rats and timed pregnant Wistar rats were purchased from Charles River (Broekman Instituut, Someren, The Netherlands). Pups at *days 1* (n = 2), *2* (n = 2), *5* (n = 3), and *9* (n = 3) after birth were anesthetized and subsequently killed by decapitation. Adult rats (n = 3) were anesthetized and subsequently killed by bleeding via aorta punction. Kidneys were rapidly excised, and part of the tissue was snap-frozen in liquid nitrogen and stored at −80°C; another part of the tissue was fixed during 16 h in 10% buffered formalin and embedded in paraffin. Kidneys from another group of 9-day-old rat pups were put into RNAlater immediately after excision (Ambion, Huntingdon, UK). All rats were control animals used in another study for which the committee for experimental animal procedures of the University of Amsterdam approved all applied procedures.

Human kidney specimens. Archival human renal tissue specimens were included in this study. Ten specimens of fetal kidneys of 15- to 22-wk gestational age were obtained from tissue examined after therapeutic termination of pregnancy at the Osaka Medical Center and Research Institute for Maternal and Child Health. Similarly, five specimens of fetal kidneys of 17- to 23-wk gestational age were obtained from tissue examined at the Academic Medical Center, University of Amsterdam. Samples of mature kidneys were from patients undergoing diagnostic evaluation at the Nagoya University School of Medicine, the University Medical Center Utrecht, or the Academic Medical Center at the University of Amsterdam and were studied after completion of the diagnostic procedures. Control mature human kidney specimens were taken from tumor-free, macroscopically normal portions of nephrectomy specimens of patients (n = 9) who underwent surgery because of localized renal tumors. Kidney specimens from patients with various renal diseases (n = 109; Table 1) were obtained by percutaneous renal biopsy. Research was performed according to the Code for Proper Secondary Use of Human Tissues (2004) of the Dutch Federation of Medical Research Associations (www.federa.org) and the AMC Research Code (2010). The medical ethical committees of the Osaka Medical Center and Research Institute for Maternal and Child Health and the Nagoya University School of Medicine approved the applied procedures.

Generation of CTGF riboprobe. A 542-bp cDNA fragment of rat CTGF (Genbank gi5070343 496–1037) was amplified by PCR using 5′-ATTTAGGTGACACTATAGAAGAGGCGTGTGCACTGCCAAAGAT-3′ and 5′-TAATACGACTCACTATAGGGAGAGCAGCCAGAAAGCTCAAACTTGA-3′ as sense and antisense primers, of which the underlined regions include SP6 and T7 RNA polymerase binding sequences, respectively. The amplicon was cloned, and in vitro transcrip-

Table 1. *Adult subjects examined by immunohistochemistry*

	No. of Subjects
Control (CTRL; tumor-free parts of kidneys with localized, polar carcinoma)	9
Minimal change nephrotic syndrome (MCNS)	11
Focal glomerulosclerosis (FGS)	5
Idiopathic membranous glomerulopathy (MGP)	11
IgA nephropathy (IgA NP)	38
Crescentic glomerulonephritis	17
Diabetic mellitus nephropathy (DM NP)	15
Others (lupus nephritis, membranoproliferative glomerulonephritis, myeloma kidney)	4
Total	110